



Critical review of membrane distillation performance criteria

Aoyi Luo, Noam Lior*

Department of Mechanical Engineering and Applied Mechanics, University of Pennsylvania, Philadelphia, PA 19104-6315, USA, email: luoaoyi@gmail.com (A. Luo), Tel. +1 215 898 4803; Fax: +1 215 573 6334; email: lior@seas.upenn.edu (N. Lior)

Received 23 November 2015; Accepted 21 January 2016

ABSTRACT

The number of published papers about membrane distillation (MD) has been growing exponentially and many evaluation and performance criteria are used to measure it; but, there is no established tradition or evaluation standard for them. This makes the evaluations difficult to compare, or even incomplete. This paper presents therefore a comprehensive critical review and clarification of the major evaluation criteria for the MD components and systems, aimed to offer some recommendations for their more uniform usage, provide clearer quantitative goals in research and industrial use, and to facilitate more correct and honest representations and comparisons. General description and models of MD are presented first, followed by criteria used to characterize the membranes, and performance criteria to evaluate the distillate production rate, product quality, energy efficiency (including conventional energy performance criteria and exergy performance criteria), transport process, and long-time operation. Since exergy analysis of the process is less known, a detailed example is presented.

Keywords: Membrane distillation; Membrane distillation performance criteria; Water desalination performance criteria; Exergy and energy performance; Transport criteria; Non-equilibrium thermodynamics criteria

1. Introduction

Membrane distillation (MD) is a thermally driven membrane separation process which uses transmembrane vapor pressure difference, generated by transmembrane temperature difference, as the driving force for the product vapor generation and flow. The separation membrane is hydrophobic, which thereby prevents the penetration of liquids but allows vapors to pass through it. In this process, liquid feed to be treated is heated and placed in contact with one side of the membrane directly. The other side of the membrane is kept at a lower vapor pressure by various

means, most commonly by condensation of the vapor at lower temperature (thus creating a lower vapor pressure), by flowing (sweeping) gases/vapors, or by pulling a vacuum, as described in detail in [1–3].

There are four basic types of MD membrane modules which differ in the way they condense the vapor through the membrane as shown in Fig. 1: (a) direct contact membrane distillation (DCMD), where the cooling solution is in direct contact with the membrane at the permeate side and (b) air gap membrane distillation (AGMD), where an air gap is interposed between the membrane and a condensation surface (to reduce the conductive heat transfer loss), and the vapor is condensed on the condensation surface after

*Corresponding author.

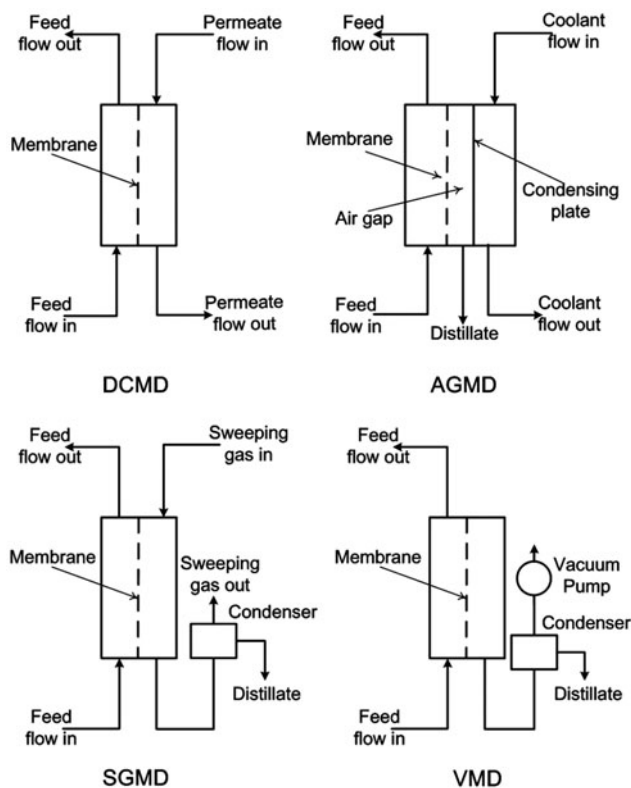


Fig. 1. Schematics of the four leading MD configurations.

crossing the air gap, (c) sweeping gas membrane distillation (SGMD), where a sweeping gas is used to drive the vapor out of the membrane module and then condensed outside, (d) vacuum membrane distillation (VMD), where vacuum is applied in the permeate side of the membrane module which carries the vapor outside of the membrane module and condensed outside.

MD promises to have many advantages in comparison with other desalination processes, including (a) a high separation factor of non-volatile solute so that it can produce high purity distillate, about 30-fold higher than RO, (b) mostly uses relatively low temperature (currently typ. $<90^{\circ}\text{C}$) rather than mechanical power that is of high exergy, cost, and environmental emissions, (c) operation at much lower pressure (around atmospheric (0.1 MPa) or below) when compared with reverse osmosis (RO, conducted at about 2.5–8.5 MPa, increasing with feedwater concentration), (d) low driving temperature that allows use of low-grade waste heat and/or renewable energy sources such as solar and geothermal, (e) less sensitivity to concentration polarization and fouling than other membrane separation processes such as RO [1,4,5], and (f) high compactness and low weight. It has

various and increasing applications, including water desalination, wastewater treatment, and several in biomedical, food, and fermentation industries [4,6–10].

These promising aspects of MD have fostered increasing R&D and publications addressing membrane materials, configurations and fabrication, transport phenomena, analysis and modeling, membrane scaling and fouling, system heat recovery, module and system design, applications, and long-time operation. Many evaluation and performance criteria are necessary for these studies and projects, some based on fundamental aspects of the process and some on specific applications and needs. Since there is no evaluation standard, the authors often used criteria developed independently, which makes it difficult to effectively compare results, or which may be incomplete for the feature of interest, or, in the worst case, may be misleading both for the fundamental aspects and for use in system design, industrial use, and system representation. The deficiencies are especially in exergy analysis and evaluation of long-term operation. This paper thus presents a comprehensive critical review and clarification of the MD component and system major evaluation criteria, aimed to offer some recommendations for their more uniform usage, to provide clearer quantitative goals in research and industrial use, and to facilitate more correct and honest representation. This review of commonly used criteria in MD is classified according to their evaluation objects and application level, with discussion about their advantages and limitations.

Brief descriptions of the different fundamental and applied aspects of MD are provided, to the extent needed for clarifying the performance criteria. Detailed explanations of the process can be found in the books and reviews including [2,4,5,9,11].

As to the format and style of this review, it is aimed both to guide those who are learning about the process, and is therefore somewhat didactic, and to serve as a reference for the practitioner and is thus formatted to allow examination of individual performance criteria without having to read the entire paper.

2. MD process and systems description

2.1. Hydrophobicity of the membrane

Hydrophobicity of the membrane is an indispensably required feature of MD, since the membrane sustains the liquid/gas interface and prevents liquid from penetrating it. The pressure difference across the membrane must not exceed its mechanical strength, its compaction that would excessively close the pores,

and the liquid entry pressure (LEP) defined as the critical transmembrane pressure difference that membrane hydrophobicity could sustain, where a larger pressure difference will result in solution penetrating the membrane as illustrated in Fig. 2. LEP for the membrane can to first approximation be calculated from the Laplace equations:

$$LEP = \Delta P_{inter} = \frac{-2B\gamma_L \cos \theta}{r_{max}} \quad (1)$$

where LEP is liquid entry pressure (Pa), ΔP_{inter} —pressure difference at the liquid/gas interface (Pa), B —geometric factor (dimensionless), γ_L —liquid surface tension (N/m), θ —membrane/liquid contact angle ($^\circ$ or rad), r_{max} —largest pore radius (m).

B is a factor determined by the geometric structure of the pore, and for a cylindrical pore, the geometric factor (B) equals to 1 [5].

2.2. Heat transfer

In MD, the heat transfer across the membrane has two paths, one is the sensible heat conduction through the membrane material and the gas within the membrane pores, and the other is the latent heat of evaporation associated with the mass flux. The sensible heat transferred is regarded as an energy loss because it has negligible contribution to the vapor mass flux.

The heat transfer in MD can be split into stages. In DCMD, the heat first is transferred across the feed stream boundary layer:

$$q_f'' = h_f(T_f - T_{f,m}) \quad (2)$$

where q_f'' is heat flux across the feed stream boundary layer (W/m^2), h_f —convective heat transfer coefficient

of the feed stream ($W/(m^2 K)$), T_f —temperature of the feed bulk (K), $T_{f,m}$ —temperature at the membrane feed-side surface (K).

Then heat is transferred across the membrane by conduction and latent heat of evaporation:

$$q_{mem}'' = J\Delta H_{fg} + h_m(T_{f,m} - T_{p,m}) = H_m(T_{f,m} - T_{p,m}) \quad (3)$$

where q_{mem}'' is heat flux across the membrane (W/m^2), J —mass flux ($kg/(m^2 s)$), h_m —conduction heat transfer coefficient of the membrane ($W/(m^2 K)$), ΔH_{fg} —specific enthalpy of vaporization (J/kg), $T_{f,m}$ —temperature at the membrane feed-side surface (K), $T_{p,m}$ —temperature at the membrane permeate-side surface (K), H_m —total heat transfer coefficient of the membrane ($W/(m^2 K)$).

Here, we define the total heat transfer coefficient of the membrane (H_m) which combines the heat transfer of conduction and evaporation as:

$$H_m = \frac{q_{mem}''}{T_{f,m} - T_{p,m}} = \frac{J\Delta H_{fg} + h_m(T_{f,m} - T_{p,m})}{T_{f,m} - T_{p,m}} \quad (4)$$

Then heat is transferred across the permeate stream boundary layer:

$$q_p'' = h_p(T_{p,m} - T_p) \quad (5)$$

where q_p'' is the heat flux across the permeate stream boundary layer (W/m^2), h_p —convective heat transfer coefficient of the permeate stream ($W/(m^2 K)$), T_p —temperature of the permeate bulk (K).

At steady state, and ignoring heat transfer from the membrane or module periphery:

$$q_t'' = q_f'' = q_{mem}'' = q_p'' \quad (6)$$

where q_t'' is total heat flux (W/m^2).

The temperature profile in DCMD is thus shown in Fig. 3. According to Eqs. (2)–(6), the total heat flux is calculated by:

$$q_t'' = \frac{T_f - T_p}{\frac{1}{h_f} + \frac{1}{H_m} + \frac{1}{h_p}} \quad (7)$$

Considering the heat transfer resistances analog in DCMD, the driving force is the temperature difference ($T_f - T_p$). The resistances are the heat transfer resistance of the feed stream ($1/h_f$), the membrane ($1/H_m$),

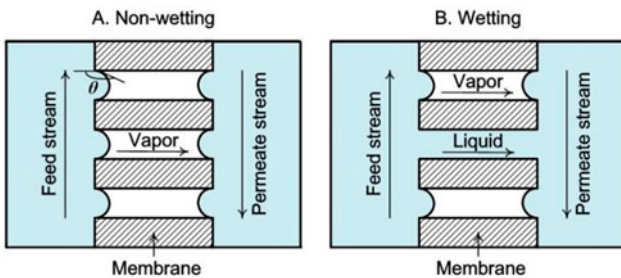


Fig. 2. Schematic of the DCMD process with a non-wetting membrane (on the left) and a membrane having a wetted pore (right).

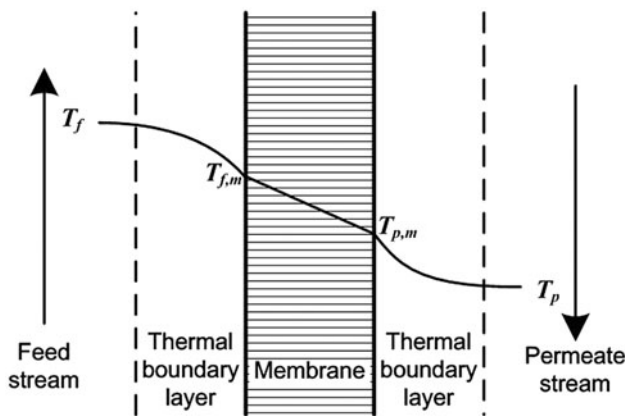


Fig. 3. The temperature profile in DCMD.

and the permeate stream ($1/h_p$) in series, as shown in Fig. 4.

For AGMD, additional heat transfer resistances caused by the air gap (R_g), the condensate thin film (R_f), and the cooling plate (R_c) are present and the method to calculate their values can be found in [8]. The total heat flux can thus be calculated by:

$$q_t'' = \frac{T_f - T_p}{\frac{1}{h_f} + \frac{1}{H_m} + R_g + R_f + R_c + \frac{1}{h_p}} \quad (8)$$

where R_g is heat transfer resistance of the air gap ($(m^2 K)/W$), R_f —heat transfer resistance of the condensate thin film ($(m^2 K)/W$), R_c —heat transfer resistance of the cooling plate ($(m^2 K)/W$).

The temperature profile in AGMD is shown in Fig. 5 and the heat transfer resistance analog in AGMD is shown in Fig. 6.

In SGMD and VMD, the vapor is condensed by an external condenser (Fig. 1), so the heat flux balance of

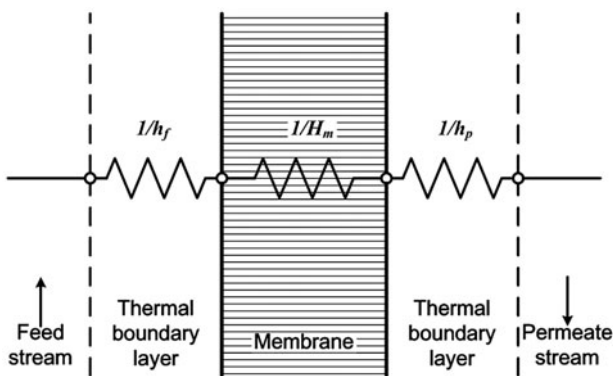


Fig. 4. The heat transfer resistance analog in DCMD.

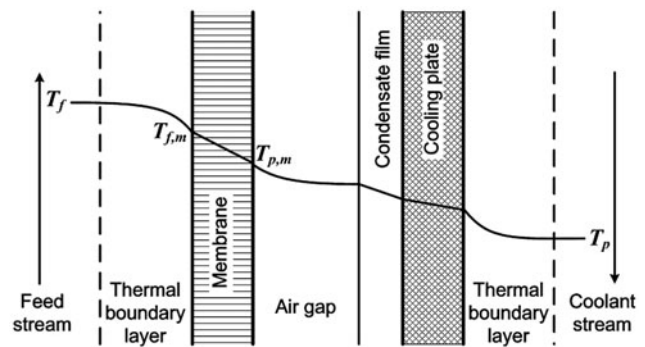


Fig. 5. The temperature profile in AGMD.

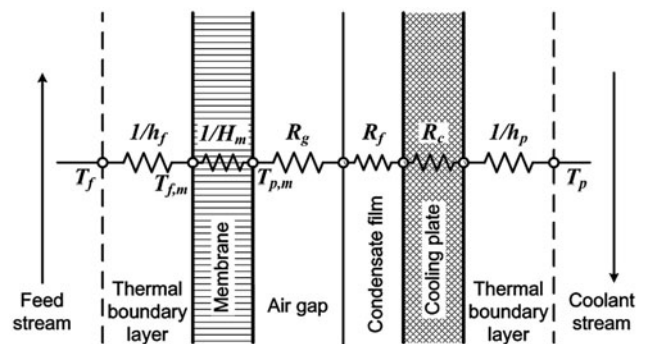


Fig. 6. The heat transfer resistance analog in AGMD.

Eq. (6) does not hold and must be developed based on the specific system configuration.

2.3. Mass transfer

The mass flux (J) across the membrane (the term mass flux is used here to denote the flux of the distillate across a membrane) is generally calculated by:

$$J = C(p_{f,m} - p_{p,m}) \quad (9)$$

where C is membrane permeability ($kg/(m^2 s Pa)$), $p_{f,m}$ —apor pressure at the membrane feed-side surface (Pa), $p_{p,m}$ —vapor pressure at the membrane permeate-side surface (Pa).

The vapor pressure of the solution can be calculated by:

$$p = p^* \cdot a \quad (10)$$

where p is vapor pressure of the solution (Pa), p^* —vapor pressure of pure solvent (Pa), a —activity of the solvent (dimensionless).

The activity (a) accounts for the deviations from ideal behavior of chemical substances in a mixture. It can be calculated by:

$$a = \gamma x \quad (11)$$

where γ is activity coefficient (dimensionless), x —mole fraction (dimensionless).

The value of activity coefficient (γ) can be estimated from experimental data or models. The data of the activity coefficients of various solutions have been reported in [12]. The models by Pitzer and co-workers [13,14] were recommended in [14] as the most accurate for predicting the activity coefficients while many other simpler models are applicable to some specific conditions and are described in [15–17].

To determine the mass flux, the dusty gas model is the most general model for flux through porous media [5]. Three mass transport mechanisms are generally considered in MD [5] and the mass transfer resistance corresponding to these three mechanisms is shown in Fig. 7. The mass flux can be decomposed into the sum of the convection flux and the diffusion flux. The convection flux is driven by the total pressure gradient where the mass transfer resistance is represented by the viscous flow model. The diffusion flux is driven by the concentration gradient (or the partial pressure gradient) where the mass transfer resistance is represented by the Knudsen model (which represents the mass transfer resistance due to molecule-to-wall collisions) and/or the ordinary molecular diffusion model (which represents the mass transfer resistance due to inter-molecule collisions).

The general mass transfer resistance analog is shown in Fig. 7, but one or more mass transfer resistances may be negligible for a specific MD process, and the Knudsen number (Kn) provides a guideline in determining the relative importance of these mechanisms as described further down. The Knudsen number is defined as:

$$Kn = \frac{\lambda}{2r} \quad (12)$$

where Kn is Knudsen number (dimensionless), λ —mean free path of vapor (m), r —average pore radius (m).

The mean free path of molecule (λ) is the average distance traveled by molecules between collisions and can be calculated from kinetic theory [5]:

$$\lambda = \frac{k_B T}{P\sqrt{2}\pi\sigma^2} \quad (13)$$

where k_B is Boltzman constant (J/K), σ —collision diameter of the molecule (m), T —temperature (K), P —pressure (Pa).

For membranes with pores smaller than the vapor free path ($Kn > 1$) where molecule-to-wall collisions dominate and the continuum approach does not hold, the dominant mass transport mechanism is the Knudsen mechanism characterized by:

$$J = \frac{2}{3} \frac{r\varepsilon}{\tau\delta} \left(\frac{8M}{\pi RT_{mem}} \right)^{\frac{1}{2}} (p_{f,m} - p_{p,m}) \quad (14)$$

where r is average pore radius (m), ε —membrane porosity (dimensionless), δ —membrane thickness (m), τ —membrane tortuosity (dimensionless), M —molecular weight of vapor (kg/mol), R —ideal gas constant (J/(mol K)), T_{mem} —average temperature in the membrane (K).

For membranes with pores bigger than the vapor free path ($Kn < 0.01$) where the continuum approach holds, two mechanisms may dominate. The ordinary molecular diffusion model represents the diffusion of the vapor flux through stationary air driven by the concentration gradient across membrane. This mechanism dominates when air is presented in the membrane pores and both sides of the membrane are kept at same total pressure, and the mass flux can be calculated by:

$$J = \frac{\varepsilon}{\tau\delta} \frac{DM}{RT_{mem}} \frac{P_{mem}}{p_{air}} (p_{f,m} - p_{p,m}) \quad (15)$$

where D is diffusion coefficient for vapor (m^2/s), P_{mem} —average total pressure in the membrane (Pa), p_{air} —average partial pressure of the non-condensable gas in the membrane (Pa).

The viscous flow model (Poiseuille flow) represents the convective flux across the membrane, driven by the total pressure gradient. This mechanism dominates for the case when one side of membrane has lower pressure than the other side and air is not present (degassed process). In this case, the flux can be calculated by:

$$J = \frac{1}{8\mu} \frac{r^2 \varepsilon M p_{mem}}{\tau\delta RT_{mem}} (P_{f,m} - P_{p,m}) \quad (16)$$

where μ is viscosity of vapor (Pa s), P_{mem} —average vapor pressure in the membrane (Pa), $P_{f,m}$ —total pressure at the membrane feed-side surface (Pa), $P_{p,m}$ —total pressure at the membrane permeate-side surface (Pa).

When $0.01 < Kn < 1$ and both sides of the membrane are kept at the same total pressure, both the inter-molecular collisions and molecule-to-wall collisions cannot be neglected. So the mass transfer mechanism is in the transition region between the Knudsen and the ordinary diffusion mechanism, and the mass transfer resistances of both the Knudsen and the ordinary diffusion mechanism must be included as shown in Fig. 7 and the mass flux is calculated by:

$$J = \left\{ \left[\frac{2 r \varepsilon}{3 \tau \delta} \left(\frac{8M}{\pi RT_{mem}} \right)^{\frac{1}{2}} \right]^{-1} + \left(\frac{\varepsilon}{\tau \delta} \frac{DM P_{mem}}{RT p_{air}} \right)^{-1} \right\}^{-1} (p_{f,m} - p_{p,m}) \tag{17}$$

2.4. Non-equilibrium thermodynamics of the transport process

Non-equilibrium thermodynamics has been applied to membrane separation processes [18] and MD [19,20]. Following this approach, the Onsager phenomenological relations between fluxes and forces in their linear form are:

$$J_j = \sum_k L_{jk} X_k \tag{18}$$

where J_j —fluxes, L_{jk} —kinetic (phenomenological) coefficients, X_k —driving forces.

The kinetic coefficients satisfy the Onsager reciprocal relationships:

$$L_{jk} = L_{kj} \tag{19}$$

In MD, the major fluxes are those of heat (here $j = 1$) and of the solvent ($j = 2$), and the major driving forces

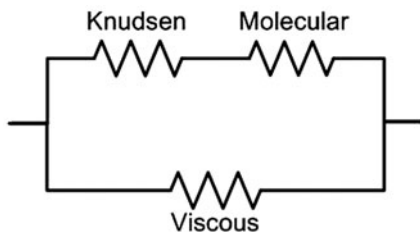


Fig. 7. The mass transfer resistance analog across a membrane.

are the temperature and the chemical potential gradients. The entropy generation rate is used to identify the forces and fluxes, and can be represented by:

$$\dot{s} = q_t'' \nabla \left(\frac{1}{T} \right) - J T^{-1} \nabla \mu \tag{20}$$

where \dot{s} is entropy production rate ($W/(K m^3)$), q_t'' —total heat flux (W/m^2), T —temperature (K), J —mass flux ($kg/(m^2 s)$), μ —chemical potential of the solution (J/kg).

Thus the fluxes and forces are:

$$J_1 \equiv q_t'' \text{ and } J_2 \equiv -J \tag{21}$$

$$X_1 \equiv \nabla \left(\frac{1}{T} \right) \text{ and } X_2 \equiv T^{-1} \nabla \mu \tag{22}$$

Substituting these terms into Eq. (18) yields the following expressions for the 2 fluxes:

$$q_t'' = L_{11} \nabla \left(\frac{1}{T} \right) + L_{12} T^{-1} \nabla \mu = -L_{11} T^{-2} \nabla T + L_{12} T^{-1} \nabla \mu \tag{23}$$

$$-J = L_{21} \nabla \left(\frac{1}{T} \right) + L_{22} T^{-1} \nabla \mu = -L_{21} T^{-2} \nabla T + L_{22} T^{-1} \nabla \mu \tag{24}$$

where L_{11} is inverse temperature-driven heat flux kinetic coefficient ($(K W)/m$), L_{12} —chemical potential-driven heat flux kinetic coefficient ($(K kg)/(m s)$), L_{21} —inverse temperature-driven mass flux kinetic coefficient ($(K kg)/(m s)$), L_{22} —chemical potential-driven mass flux kinetic coefficient ($(K kg^2)/(m s J)$).

Knowledge of the imposed driving forces and of the kinetic coefficients thus allows calculations of the fluxes and thus solution of the problem. A procedure to calculate the latter is outlined below. Using Eqs. (3), (6), and (24):

$$q_t'' = -h_m \nabla T + J \Delta H_{fg} = (-h_m + \Delta H_{fg} L_{21} T^{-2}) \nabla T - \Delta H_{fg} L_{22} \nabla \mu \tag{25}$$

where h_m is conduction heat transfer coefficient of the membrane ($W/(m^2 K)$), ΔH_{fg} —specific enthalpy of vaporization (J/kg).

Using Eqs. (23) and (25) give:

$$L_{11} = -h_m T^2 + \Delta H_{fg} L_{21} \tag{26}$$

$$L_{12} = -\Delta H_{fg} L_{22} \quad (27)$$

To derive the kinetic coefficient expressions, first consider the case in which the mass flux is driven only by the temperature gradient, holding the chemical potential to be same at both sides of the membrane.

Using:

$$J = C(p_{f,m} - p_{p,m}) \quad (28)$$

where C is membrane permeability ($\text{kg}/(\text{m}^2 \text{ s Pa})$), $p_{f,m}$ —vapor pressure at the membrane feed-side surface (Pa), $p_{p,m}$ —vapor pressure at the membrane permeate-side surface (Pa).

and assuming here for simplicity that:

$$\nabla T \approx \frac{T_{p,m} - T_{f,m}}{\delta} \text{ and } \nabla \mu \approx \frac{\mu_{p,m} - \mu_{f,m}}{\delta} \quad (29)$$

where δ is membrane thickness (m), $T_{f,m}$ —temperature at the membrane feed-side surface (K), $T_{p,m}$ —temperature at the membrane permeate-side surface (K), $\mu_{f,m}$ —chemical potential of the solution at the membrane feed-side surface (J/kg), $\mu_{p,m}$ —chemical potential of the solution at the membrane permeate-side surface (J/kg).

Eqs. (10), (28) and (29) lead to:

$$J = -C\delta \frac{a_{me}(p_{f,m}^* - p_{p,m}^*)}{T_{f,m} - T_{p,m}} \frac{T_{p,m} - T_{f,m}}{\delta} \approx -C\delta a_{me} \left[\frac{\partial p^*}{\partial T} (T_{me}) \right]_{\mu} \nabla T \quad (30)$$

where a_{me} —mean activity of both sides of the membrane surface (dimensionless), $p_{f,m}^*$ —vapor pressure of pure solvent at the membrane feed-side surface (Pa), $p_{p,m}^*$ —vapor pressure of pure solvent at the membrane permeate-side surface (Pa), T_{me} —mean temperature of both sides of the membrane surface (K).

Eqs. (24) and (30) lead to:

$$L_{21} = -C\delta T^2 a_{me} \frac{p_{f,m}^* - p_{p,m}^*}{T_{f,m} - T_{p,m}} \approx -C\delta T^2 a_{me} \left[\frac{\partial p^*}{\partial T} (T_{me}) \right]_{\mu} \quad (31)$$

As the second step, consider the case in which the mass flux is driven only by the chemical potential gradient, holding the temperature to be the same at both sides of the membrane, and Eq. (28) leads to:

$$J = -C\delta \frac{p_{f,m} - p_{p,m}}{\mu_{f,m} - \mu_{p,m}} \frac{\mu_{p,m} - \mu_{f,m}}{\delta} \approx -C\delta \left[\frac{\partial p}{\partial \mu} (\mu_{me}) \right]_T \nabla \mu \quad (32)$$

Eqs. (24) and (32) lead to:

$$L_{22} = C\delta T \frac{p_{f,m} - p_{p,m}}{\mu_{f,m} - \mu_{p,m}} \approx C\delta T \left[\frac{\partial p}{\partial \mu} (\mu_{me}) \right]_T \quad (33)$$

where μ_{me} is mean chemical potential of the solution at both sides of the membrane surface (J/kg).

Since

$$\mu_{f,m} - \mu_{p,m} = R_v T \ln \frac{a_{f,m}}{a_{p,m}} \approx R_v T \left(\frac{\partial \mu}{\partial a} \right)_T = \frac{R_v T}{a_{me}} (a_{f,m} - a_{p,m}) \quad (34)$$

$$p_{f,m} - p_{p,m} = p^* (a_{f,m} - a_{p,m}) \quad (35)$$

According to Eqs. (33)–(35):

$$L_{22} = C\delta \frac{p^* (a_{f,m} - a_{p,m})}{R_v (\ln a_{f,m} - \ln a_{p,m})} \approx \frac{C\delta p^* a_{me}}{R_v} \quad (36)$$

where $a_{f,m}$ is activity at the membrane feed-side surface (dimensionless), $a_{p,m}$ —activity at the membrane permeate-side surface (dimensionless), R_v —gas constant of vapor (J/(kg K)), calculated by:

$$R_v = \frac{R}{M} \quad (37)$$

where R is ideal gas constant (J/(mol K)), M —molecular weight of vapor (kg/mol).

Using Eqs. (27) and (36), lead to:

$$L_{12} = -\Delta H_{fg} C\delta \frac{p^* (a_{f,m} - a_{p,m})}{R_g (\ln a_{f,m} - \ln a_{p,m})} \approx -\Delta H_{fg} \frac{C\delta p^* a_{me}}{R_g} \quad (38)$$

From the Clausius–Clapeyron equation:

$$\Delta H_{fg} = \frac{R_v T^2}{p^*} \left[\frac{\partial p}{\partial T} (T_{me}) \right]_{\mu} \quad (39)$$

Using Eqs. (31), (38), and (39), the Onsager reciprocal relationship yields:

$$L_{12} = -C\delta T^2 a_{me} \left[\frac{\partial p}{\partial T} (T_{me}) \right]_{\mu} = L_{21} \quad (40)$$

According to Eqs. (26) and (31):

$$L_{11} = -h_m T^2 - \Delta H_{fg} C\delta \left[\frac{\partial p}{\partial T} (T_{me}) \right]_{\mu} T^2 \quad (41)$$

The four kinetic coefficients can be simplified to be expressed as:

$$L'_{11} = -L_{11}/T^2 = h_m + \Delta H_{fg} C\delta \left[\frac{\partial p}{\partial T} (T_{me}) \right]_{\mu} \quad (42)$$

$$L'_{21} = L_{21}/T^2 = -C\delta a_{me} \left[\frac{\partial p}{\partial T} (T_{me}) \right]_{\mu} \quad (43)$$

$$L'_{12} = \left(\frac{\partial \mu}{\partial c} \right)_T L_{12}/T = -\Delta H_{fg} C\delta p^* \left(\frac{\partial a}{\partial c} \right)_T \quad (44)$$

$$L'_{22} = -\left(\frac{\partial \mu}{\partial c} \right)_T L_{22}/T = -C\delta p^* \left(\frac{\partial a}{\partial c} \right)_T \quad (45)$$

where c is volumetric molar concentration (mol/m^3).

Substituting Eqs. (42)–(45) into Eqs. (23) and (24), the two fluxes can thus be expressed as:

$$q'_i = L'_{11} \nabla T + L'_{12} \nabla c \quad (46)$$

$$J = L'_{21} \nabla T + L'_{22} \nabla c \quad (47)$$

where L'_{11} is temperature-driven heat flux kinetic coefficient ($\text{W}/(\text{m K})$), L'_{12} —concentration-driven heat flux kinetic coefficient ($(\text{W m}^2)/\text{mol}$), L'_{21} —temperature-driven mass flux kinetic coefficient ($(\text{kg K})/(\text{m s})$), L'_{22} —concentration-driven mass flux kinetic coefficient ($(\text{kg m}^2)/(\text{mol s})$).

All the kinetic coefficients can be determined from experiments or simulations based on the chosen process conditions.

It is noteworthy that the kinetic coefficients are also a form of process performance criteria, since they

represent the relationship between the given driving forces and the resulting fluxes.

2.5. Energy analysis

While heat is consumed in the coupled mass and heat transfer process across the membrane, and is also lost to the environment, typical practical use includes many other auxiliary energy-consuming units which consume not only heat but also electrical energy, such as those used for pumping, pre- and post-treatment, disposal of wastes, instrumentation, control, and plant operations such as lighting, HVAC, security, and such.

As in all desalination processes, integration of heat recovery is critical for the successful commercial use of MD and must thus be included in the energy analysis. A simple demonstration of this issue is that the heat required for water evaporation is about 2,400 kJ/kg while the minimal energy required for the separation of water from 3.5% salinity seawater is only about 3 kJ/kg [21]. Since the produced vapor must be condensed, the heat of condensation accounts for much of the huge energy demand difference between these values, and is therefore typically used for preheating the feed solution and thus “recovering” some of the invested heat and thereby reducing the heat demand. Current practice in thermal water desalination processes uses performance ratios (PRs) of about 8 to 30, i.e. only 1/30–1/8 of the latent heat must be expended. Fig. 8 shows a DCMD system with heat recovery. For a system as Fig. 8 shows and neglect the energy and mass losses to the environment, the energy balance yields:

$$\dot{H}_{in,f} + \dot{H}_{in,p} + \dot{W}_{e,f} + \dot{W}_{e,p} + \dot{Q}_{in} = \dot{H}_{out,f} + \dot{H}_{out,p} \quad (48)$$

where $\dot{H}_{in,f}$ is enthalpy of the feed inflow (W), $\dot{H}_{in,p}$ —enthalpy of the permeate inflow (W), $\dot{W}_{e,f}$ —electrical energy consumption of the feed flow pump (W), $\dot{W}_{e,p}$ —electrical energy consumption of the permeate flow pump (W), \dot{Q}_{in} —heat input rate (W), $\dot{H}_{out,f}$ —enthalpy of the feed outflow (W), $\dot{H}_{out,p}$ —enthalpy of the permeate outflow (W).

and the mass balance yields

$$\dot{m}_{in,f} + \dot{m}_{in,p} = \dot{m}_{out,f} + \dot{m}_{out,p} \quad (49)$$

where $\dot{m}_{in,f}$ is mass inflow rate of the feed solution (kg/s), $\dot{m}_{in,p}$ —mass inflow rate of the permeate (kg/s), $\dot{m}_{out,f}$ —mass outflow rate of the feed solution (kg/s), $\dot{m}_{out,p}$ —mass outflow rate of the permeate (kg/s).

We now describe the energy and mass balance of the membrane module and the heat exchanger (in dashed-line box of Fig. 8), and implement the typical neglect of energy and mass losses to the environment, and of mass transfer in the heat exchanger. In the membrane module, the heat and mass are transferred across the membrane from the feed stream to the permeate stream, thus the energy and mass balance of the membrane module yield:

$$\dot{H}_{in,f}^m - \dot{H}_{out,f}^m = \dot{H}_{out,p}^m - \dot{H}_{in,p}^m = q_t'' A \quad (50)$$

where $\dot{H}_{in,f}^m$ is enthalpy of the feed inflow to the membrane module (W), $\dot{H}_{out,f}^m$ —enthalpy of the feed outflow from the membrane module (W), $\dot{H}_{out,p}^m$ —enthalpy of the permeate outflow from the membrane module (W), $\dot{H}_{in,p}^m$ —enthalpy of the permeate inflow to the membrane module (W), q_t'' —total heat flux across membrane (W/m²), A —membrane area (m²).

$$\dot{m}_{in,f}^m - \dot{m}_{out,f}^m = \dot{m}_{out,p}^m - \dot{m}_{in,p}^m = JA \quad (51)$$

where $\dot{m}_{in,f}^m$ is mass inflow rate of the feed solution to the membrane module (kg/s), $\dot{m}_{out,f}^m$ —mass outflow rate of the feed solution from the membrane module (kg/s), $\dot{m}_{out,p}^m$ —mass outflow rate of the permeate from the membrane module (kg/s), $\dot{m}_{in,p}^m$ —mass inflow rate of the permeate to the membrane module (kg/s), J —mass flux (kg/(m² s)).

The energy and mass balance of the heat exchanger yield:

$$\dot{H}_{in,f}^h - \dot{H}_{out,f}^h = \dot{H}_{out,p}^h - \dot{H}_{in,p}^h = \dot{Q}_r \quad (52)$$

where $\dot{H}_{in,f}^h$ is enthalpy of the feed inflow to the heat exchanger (W), $\dot{H}_{out,f}^h$ —enthalpy of the feed outflow from the heat exchanger (W), $\dot{H}_{out,p}^h$ —enthalpy of the permeate outflow from the heat exchanger (W), $\dot{H}_{in,p}^h$ —enthalpy of the permeate inflow to the heat exchanger (W), \dot{Q}_r —heat recovery rate (W).

$$\dot{m}_{in,f}^h = \dot{m}_{out,f}^h \text{ and } \dot{m}_{out,p}^h = \dot{m}_{in,p}^h \quad (53)$$

where $\dot{m}_{in,f}^h$ is mass inflow rate of the feed solution to the heat exchanger (kg/s), $\dot{m}_{out,f}^h$ —mass outflow rate of the feed solution from the heat exchanger (kg/s), $\dot{m}_{out,p}^h$ —mass outflow rate of the permeate from the heat exchanger (kg/s), $\dot{m}_{in,p}^h$ —mass inflow rate of the permeate to the heat exchanger (kg/s).

Many of the thermal desalination plants are designed as dual-purpose ones, where the high grade

input energy is used for a power plant, and the lower grade rejected from the power plant is used to operate an MSF or MED desalination plant, thus generating both power and water [22–26]. The rejected heat can similarly be used to operate an MD plant. Compared with single-purpose power plants, dual purpose plants sacrifice some power generation capacity to the benefit of water production, and dual-purpose plants are typically more economical and have somewhat less negative impact on the environment than separate power-only and water-only systems [22]. Fig. 9 shows a dual-purpose desalination plant where the MD system shown in Fig. 8 is coupled with a vapor power system. The two systems are coupled by the condenser of the vapor power system where the low grade rejected heat is transferred from the power system to the MD system. Neglecting the plant's energy loss to the environment, the energy balance of the MD system is the same as shown in Eq. (48) except that the heat input (\dot{Q}_{in}) in Eq. (48) is now replaced by the heat exchanged in the condenser (\dot{Q}_c). The energy balance of the vapor power system yields:

$$\dot{Q}_{fuel} + \dot{W}_{e,w} = \dot{Q}_c + \dot{W}_{e,t} \quad (54)$$

where \dot{Q}_{fuel} is heat input rate by the fuel (W), $\dot{W}_{e,w}$ —electrical energy consumption of the water pump (W), \dot{Q}_c —heat exchange rate in the condenser (W), $\dot{W}_{e,t}$ —electrical energy output of the vapor power system (W).

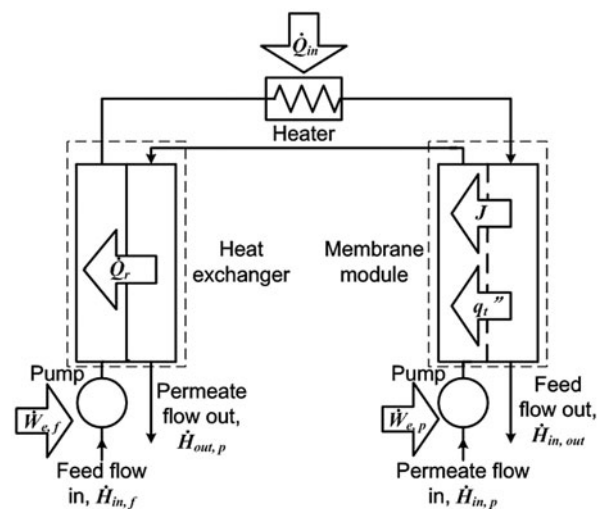


Fig. 8. Schematic of a DCMD system with heat recovery (dashed lines denote the control volume of the membrane module and heat exchanger).

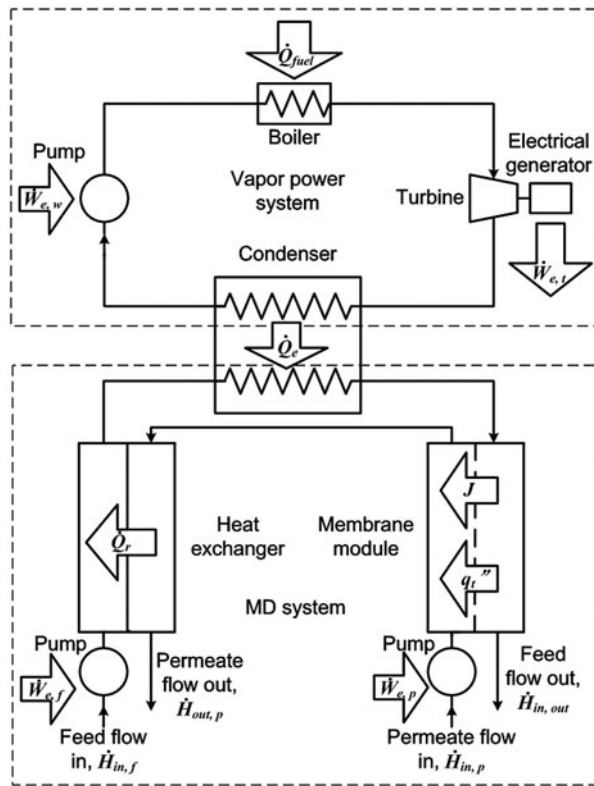


Fig. 9. Schematic of a dual purpose desalination plant (dashed lines denote the MD system and vapor power plant).

The energy balance of the dual-purpose desalination plant according to Eqs. (48) and (54) thus yields:

$$\begin{aligned} \dot{H}_{in,f} + \dot{H}_{in,p} + \dot{W}_{e,f} + \dot{W}_{e,p} + \dot{Q}_{fuel} + \dot{W}_{e,w} \\ = \dot{H}_{out,f} + \dot{H}_{out,p} + \dot{W}_{e,t} \end{aligned} \quad (55)$$

2.6. Exergy analysis

As stated in the above discussion about energy analysis in MD, different qualities of energy (thermal, mechanical, chemical...) are involved in the MD process but energy analysis (that is by definition based on the first law of thermodynamics) does not distinguish between them. Exergy analysis based on the second law of thermodynamics taking into account the quality of energy provides a more appropriate measure of the effectiveness of the energy use and evaluates the irreversibilities in the process. Exergy is defined as the maximal theoretical useful work a system can produce as it comes into equilibrium with its environment, or the minimal work that needs to be supplied as a

system undergoes a process between initial and final equilibrium states.

Generally, the exergy input and output involved in MD process are exergy of thermal and electrical energy and flow exergy. For exergy of thermal and electrical energy, they can be calculated by:

$$\dot{E}_{thermal} = \dot{Q} \left(1 - \frac{T}{T_0} \right) \quad (56)$$

$$\dot{E}_{electrical} = \dot{W}_e \quad (57)$$

where $\dot{E}_{thermal}$ is rate of the thermal exergy transferred (W), \dot{Q} —rate of the heat transferred (W), T —temperature (K), T_0 —dead state temperature (K), $\dot{E}_{electrical}$ —rate of the electrical exergy transferred (W), \dot{W}_e —rate of the electrical energy transferred (W).

For flow exergy, since MD can treat various solutions such as sea water, brines with high salinity, wastewater and food solution, a general method to calculate the flow exergy is needed (e.g. [15,27]). The flow exergy can be decomposed into physical exergy (thermal, pressure, velocity, and elevation) and chemical exergy:

$$\dot{E}_{flow} = \dot{E}^P + \dot{E}^C \quad (58)$$

where \dot{E}_{flow} is rate of the flow exergy transferred (W), \dot{E}^P —rate of the physical exergy transferred (W), \dot{E}^C —rate of the chemical exergy transferred (W).

The physical exergy can be calculated by:

$$\dot{E}^P = \dot{m} \left[H - H_0 - T_0(s - s_0) + \frac{v^2}{2} + g(z - z_0) \right] \quad (59)$$

where \dot{m} is mass flow rate (kg/s), H —specific enthalpy (J/kg), H_0 —specific enthalpy at dead state (J/kg), T_0 —dead state temperature (K), s —specific entropy (J/(K kg)), s_0 —specific entropy at dead state (J/(K kg)), v —velocity (m/s), g —gravitational acceleration (m/s²), z —height (m), z_0 —dead state height (m).

With the kinetic and potential exergy neglected, the physical exergy of flow for incompressible fluid treated in MD can be calculated by:

$$\begin{aligned} \dot{E}^P &= \dot{m} [H - H_0 - T_0(s - s_0)] \\ &= \dot{m} \left[C_v(T - T_0) + \frac{P - P_0}{\rho} - C_p T_0 \ln \frac{T}{T_0} \right] \end{aligned} \quad (60)$$

where C_v is specific heat capacity at constant volume (J/(K kg)), C_p —specific heat capacity at constant pressure (J/(K kg)), ρ —density (kg/m³).

Generally, there is no chemical reaction in MD but only the concentration change of the species during the MD separation process. So the chemical exergy can be calculated by:

$$\dot{E}^C = \sum_i \dot{m}_i (\mu_i - \mu_{i,0}) \quad (61)$$

where \dot{m}_i is mass flow rate of species i (kg/s), μ_i —specific chemical potential of species i (J/kg), $\mu_{i,0}$ —specific chemical potential of species i at dead state (J/kg).

The difference of chemical potential can be evaluated by:

$$\mu_i(T_0, P_0, x_i) - \mu_i(T_0, P_0, x_{i,0}) = R_i T_0 \ln \frac{a_i}{a_{i,0}} \quad (62)$$

where a_i is activity of species i (dimensionless), $a_{i,0}$ —activity of species i at dead state (dimensionless), R_i —gas constant of species i (J/(kg K)), calculated by:

$$R_i = \frac{R}{M_i} \quad (63)$$

where R is ideal gas constant (J/(mol K)), M_i —molecular weight of species i (kg/mol).

Thus the chemical exergy can be calculated by:

$$\dot{E}^C = \sum_i \dot{m}_i R_i T_0 \ln \frac{a_i}{a_{i,0}} \quad (64)$$

The calculation of the activity is discussed in the previous Section 2.3.

The value of the exergy depends on the selection of the dead state (ambient conditions). For general water desalination applications, the dead state is usually chosen as $T_0 = 25^\circ\text{C}$, $p_0 = 101.325\text{ kPa}$ and solutes mass fraction $w_{s,0} = 0.035\text{ kg/kg}$. These values will be different depending on conditions such as the specific geographic location and solute composition.

Unlike energy, exergy is not conserved but destroyed in any real process, and the exergy balance yields:

$$\dot{E}_{des} = \dot{E}_{input} - \dot{E}_{output} \quad (65)$$

where \dot{E}_{input} is exergy input rate (W), \dot{E}_{output} —exergy output rate (W), \dot{E}_{des} —exergy destruction rate (W).

Fig. 10 shows a simple DCMD system. The exergy input of this DCMD system includes the flow exergy of the feed inflow ($\dot{E}_{in,f}$) and the permeate inflow ($\dot{E}_{in,p}$), the exergy of the electrical energy consumption of the feed flow pump ($\dot{W}_{e,f}$) and the permeate flow pump ($\dot{W}_{e,p}$) and the exergy of the heat consumption of the heater (\dot{Q}_{in}):

$$\dot{E}_{input} = \dot{E}_{in,f} + \dot{E}_{in,p} + \dot{W}_{e,f} + \dot{W}_{e,p} + \dot{Q}_{in} \left(1 - \frac{T_{in}}{T_0}\right) \quad (66)$$

where $\dot{E}_{in,f}$ is flow exergy of the feed inflow (W), $\dot{E}_{in,p}$ —flow exergy of the permeate inflow (W), $\dot{W}_{e,f}$ —electrical energy consumption of the feed flow pump (W), $\dot{W}_{e,p}$ —electrical energy consumption of the permeate flow pump (W), \dot{Q}_{in} —heat input rate (W), T_{in} —temperature of the heat input (K).

The exergy output of this DCMD system includes the flow exergy of the feed outflow ($\dot{E}_{out,f}$) and the permeate outflow ($\dot{E}_{out,p}$):

$$\dot{E}_{output} = \dot{E}_{out,f} + \dot{E}_{out,p} \quad (67)$$

where $\dot{E}_{out,f}$ is flow exergy of the feed outflow (W), $\dot{E}_{out,p}$ —flow exergy of the permeate outflow (W).

The exergy input of the AGMD system shown in Fig. 11 includes the flow exergy of the feed inflow ($\dot{E}_{in,f}$) and the coolant inflow ($\dot{E}_{in,c}$), exergy of the

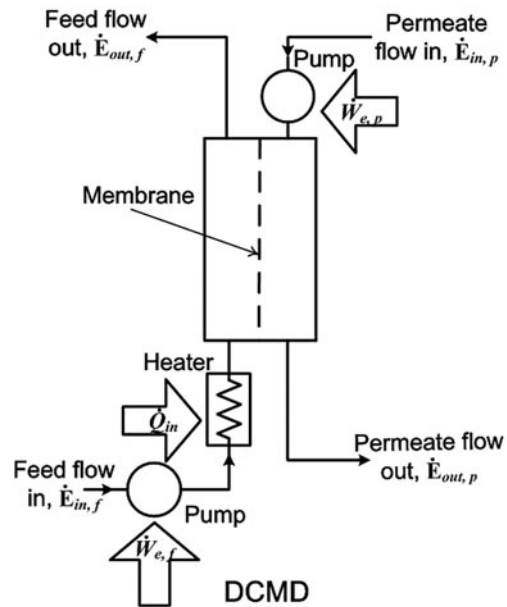


Fig. 10. Exergy analysis flow diagram of a simple DCMD system.

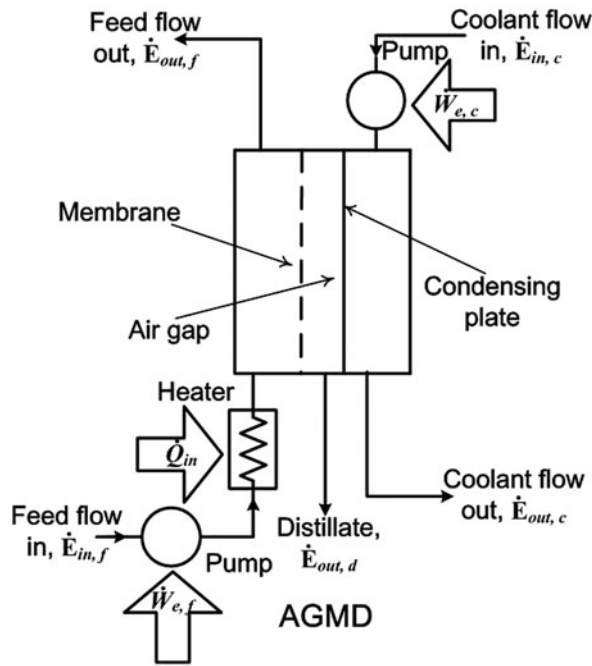


Fig. 11. Exergy analysis flow diagram of a simple AGMD system.

electrical energy consumption of the feed flow pump ($\dot{W}_{e,f}$) and the coolant flow pump ($\dot{W}_{e,c}$) and the exergy of the heat consumption of the heater (\dot{Q}_{in}).

$$\dot{E}_{input} = \dot{E}_{in,f} + \dot{E}_{in,c} + \dot{W}_{e,f} + \dot{W}_{e,c} + \dot{Q}_{in} \left(1 - \frac{T_{in}}{T_0}\right) \quad (68)$$

where $\dot{E}_{in,c}$ is flow exergy of the coolant inflow (W), $\dot{W}_{e,c}$ —electrical energy consumption of the coolant flow pump (W).

The exergy output of this AGMD system includes the flow exergy of the feed outflow ($\dot{E}_{out,f}$), the coolant outflow ($\dot{E}_{out,c}$), and the distillate ($\dot{E}_{out,d}$).

$$\dot{E}_{output} = \dot{E}_{out,f} + \dot{E}_{out,c} + \dot{E}_{out,d} \quad (69)$$

where $\dot{E}_{out,c}$ is flow exergy of the coolant outflow (W), $\dot{E}_{out,d}$ —flow exergy of the distillate (W).

The exergy input of the SGMD system shown in Fig. 12 includes the flow exergy of the feed inflow ($\dot{E}_{in,f}$) and the sweeping gas inflow ($\dot{E}_{in,g}$), the exergy of the electrical energy consumption of the feed flow pump ($\dot{W}_{e,f}$) and the sweeping gas blower ($\dot{W}_{e,b}$), and the exergy of the heat consumption of the heater (\dot{Q}_{in}).

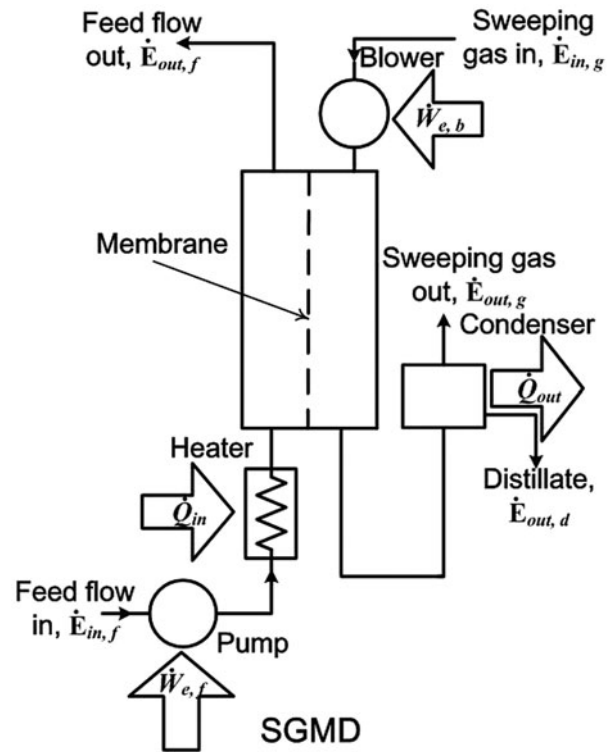


Fig. 12. Exergy analysis flow diagram of a simple SGMD system.

$$\dot{E}_{input} = \dot{E}_{in,f} + \dot{E}_{in,g} + \dot{W}_{e,f} + \dot{W}_{e,b} + \dot{Q}_{in} \left(1 - \frac{T_{in}}{T_0}\right) \quad (70)$$

where $\dot{E}_{in,g}$ is flow exergy of the sweeping gas inflow (W), $\dot{W}_{e,b}$ —electrical energy consumption of the sweeping gas blower (W).

The exergy output of this SGMD system includes the flow exergy of the feed outflow ($\dot{E}_{out,f}$), the sweeping gas outflow ($\dot{E}_{out,g}$), the distillate ($\dot{E}_{out,d}$), and the exergy of heat output of the condenser (\dot{Q}_{out}).

$$\dot{E}_{output} = \dot{E}_{out,f} + \dot{E}_{out,g} + \dot{E}_{out,d} + \dot{Q}_{out} \left(1 - \frac{T_{out}}{T_0}\right) \quad (71)$$

where $\dot{E}_{out,g}$ is flow exergy of the sweeping gas outflow (W), \dot{Q}_{out} —heat output rate (W), T_{out} —temperature of the heat output (K).

The exergy input of the VMD system shown in Fig. 13 includes the flow exergy of the feed inflow ($\dot{E}_{in,f}$), the exergy of the electrical energy consumption of the feed flow pump ($\dot{W}_{e,f}$) and the vacuum pump ($\dot{W}_{e,v}$), and the exergy of the heat consumption of the heater (\dot{Q}_{in}).

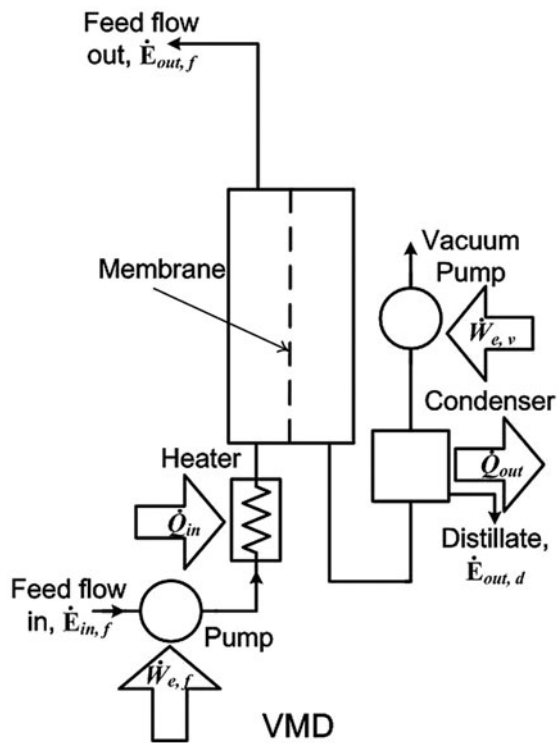


Fig. 13. Exergy analysis flow diagram of a simple VMD system.

$$\dot{E}_{input} = \dot{E}_{in,f} + \dot{W}_{e,f} + \dot{W}_{e,v} + \dot{Q}_{in} \left(1 - \frac{T_{in}}{T_0}\right) \quad (72)$$

where $\dot{W}_{e,v}$ is the electrical energy consumption of the vacuum pump (W).

The exergy output of this VMD system includes the flow exergy of the feed outflow ($\dot{E}_{out,f}$), the distillate ($\dot{E}_{out,d}$) and the exergy of heat output of the condenser (\dot{Q}_{out}).

$$\dot{E}_{output} = \dot{E}_{out,f} + \dot{E}_{out,d} + \dot{Q}_{out} \left(1 - \frac{T_{out}}{T_0}\right) \quad (73)$$

3. Performance criteria

3.1. Introduction

As in all separation and concentration processes, the ultimate goal in MD is to get maximal production (here of distillate or concentrated feed solution) rate of a product of adequate quality at the lowest lifetime cost. Since the cost is based on the sum of that of capital investment in the distillation, of energy and

operations, and of regulated environmental impacts of all, where typically the raise of the first results in a drop of the latter three, design is to be based on optimization. Reduction of energy consumption is especially important because of its costs and their sharp fluctuations, because of its significant fraction of the environmental impacts, and of depletion of non-renewable energy resources (only a negligible fraction of distillation is currently done using renewable energy).

A comprehensive evaluation of MD should therefore include at least the specific distillate production rate as a function of operating time, the energy efficiency, and the distillate quality. Also, the criteria for evaluating the transport process in MD are often useful to understand the transport process and further improvement of the MD. They can be classified into four levels based on the objects they characterize and evaluate:

- (1) The *membrane level* where the criteria are used to characterize the membrane performance independently of the rest of the system/apparatus. These criteria are often used in studies focused on the membrane itself, including membrane fabrication and modifications.
- (2) The *MD membrane module level*, where the criteria are used to evaluate the performance of the entire MD membrane module, used in membrane module analysis, modeling, design, and improvement. The membrane module is the component in which the entire distillation process takes place, which in addition to the membranes also includes the feed and the distillate streams, as well as components on the cold side of the membrane that depend on the specific design, such as an air gap, condensate liquid film, cooling plate and coolant stream in AGMD, sweeping gas in SGMD, vacuum subsystem in VMD. A qualitative schematic of the temperature profile in a DCMD membrane module is shown in Fig. 3 and of the temperature profiles in an AGMD membrane module is shown in Fig. 5.
- (3) The *MD system level* that in addition to the membrane module also includes other devices necessary for the overall distillation system operation, such as pumps, flow pipes, heat exchangers, condenser, pre- and post-treatment devices, where the criteria are used to evaluate the performance of the entire MD system. These criteria are used in the studies and evaluations such as design of multi-effect MD system, MD system coupled with other separation processes, and MD systems driven by

different energy supply system. Schematics of simple MD systems are shown in Figs. 10–13 and a schematic of a DCMD system with heat recovery is shown in Fig. 8.

- (4) The MD *long-time operation level* where the criteria are used to evaluate the performance of MD in long-time operation. These criteria are often used in researches focused on scaling, fouling, and membrane effective life.

The paper first presents the criteria used to characterize the membranes, and then the performance criteria with respect to the production rate, the product quality, the energy efficiency (including conventional energy performance criteria and exergy performance criteria), the transport process, and long-time operation.

3.2. Membrane characteristics

Membrane distillation uses hydrophobic membrane to create the interface for evaporation, and membrane properties obviously affect the process performance. The performance criteria used to characterize the membrane used in MD are discussed in this section.

3.2.1. Basic membrane properties

This subsection lists the basic properties of interest in MD.

3.2.1.1. Membrane porosity (ϵ) (dimensionless). Defined as the volume of the pores divided by the total volume of the membrane.

$$\epsilon = \frac{V_p}{V_{mem}} \quad (74)$$

where ϵ is membrane porosity (dimensionless), V_p —volume of the pores (m^3), V_{mem} —total volume of the membrane (m^3).

ϵ can also be determined by the Smolder–Franken equation [28]:

$$\epsilon = 1 - \frac{\rho_{mem}}{\rho_{mat}} \quad (75)$$

where ρ_{mem} is density of the membrane (including the pores) (kg/m^3), ρ_{mat} —density of the membrane solid matrix material (kg/m^3).

Higher porosity provides more area for evaporation, lower vapor flow resistance, and less volume of the membrane material. Also, the membrane solid matrix material has higher thermal conductivity than the gas in the pores, so higher membrane porosity results in smaller portion of the membrane solid matrix material which reduce the membrane effective thermal conductivity and transmembrane conduction heat loss as shown in Eqs. (3) and (84). At the same time, higher porosity is associated with higher pore radius and reduces the ability of the membrane to prevent liquid phase flow through it (Eq. (1)), so an optimal porosity must be selected.

3.2.1.2. Membrane thickness (δ) (m). A larger thickness leads to a smaller mass flux and smaller heat loss by conduction, since mass transfer and heat conduction resistance increase with the membrane thickness as discussed in Section 2.3 and is shown in Eq. (84).

3.2.1.3. Membrane tortuosity (τ) (dimensionless). The ratio of the average length of pores to the membrane thickness.

$$\tau = \frac{l_p}{\delta} \quad (76)$$

where τ is membrane tortuosity (dimensionless), l_p —average length of pores (m), δ —membrane thickness (m).

Larger membrane tortuosity means that the vapor flow path is longer, which results in higher mass transfer resistance, so a membrane with larger membrane tortuosity has a smaller mass flux as discussed in Section 2.3.

3.2.1.4. Membrane pore size (d_p) (m). Increasing the pore size raises the mass flux, but also increases the possibility of membrane wetting, according to the Eq. (1).

In fact, the pores in a single membrane have different sizes, characterized by a size distribution. Several technologies have been applied to determine the mean pore size and pore size distribution, including Scanning Electron Microscopy (SEM), Atomic Force Microscopy (AFM), wet/dry flow method, and gas permeation test [2] While the calculated permeability can be different when using the mean pore size instead of using the pore size distribution [29], Martinez et al. [30] found that the values are similar. It is also noteworthy that the pore sizes change with operation, due to mechanical and chemical effects, temperature changes, and fouling.

3.2.1.5. *Membrane material thermal conductivity (k_s)* ($W/(m^2 \cdot K)$). As shown in Eqs. (3) and (84), membrane material with lower heat conductivity is desirable because it results in smaller transmembrane conduction heat loss.

3.2.1.6. *Membrane/liquid contact angle (θ)* ($^\circ$ or rad). The MD process relies on the hydrophobicity of the membrane and the contact angle is a measure of the hydrophobicity. Larger contact angles are preferable to ensure the hydrophobicity and prevent feed solution from entering the pores according to the Eq. (1). It should be noted that the contact angle depends on the membrane material and on liquid composition (including even trace amounts of surfactants) and on the operating temperature.

3.2.1.7. *Membrane mechanical strength*. Generally, MD operates at around atmospheric pressure (0.1 MPa) or below, so the requirement for mechanical strength is not that high when compared with RO, but sufficient strength is still needed to prevent membranes from compacting or cracking. The mechanical strength can be estimated by tensile strength, Young's module, and burst pressure. More information about measuring the membrane mechanical properties can be found in [31].

3.2.1.8. *Membrane chemical stability*. It is commonly agreed that in MD the membrane only serves as a support of the vapor/liquid interface and is not involved in the mass transport process [4]. It must, however, be chemically stable for operation with the feed solution and foulants at the operating temperatures. Chlorine, sulfuric acid, hydrochloric acid, and sodium hydroxide solutions are most often used as test solutions to evaluate the chemical stability of the membrane. When the chemical stability is needed for a specific application, specific applicable solutions can be used as test solutions. The chemical stability can be estimated by visual comparison, change of other membrane properties such as thickness, porosity, contact angle, and tensile strength, before and after test. More information about measuring the membrane chemical stability can be found in [31].

3.2.1.9. *Membrane thermal stability*. Membranes used in MD should have good thermal stability to ensure long-time operation at the operating temperature (so far usually below 100°C). Thermal stability essays such as differential scanning calorimetry (DSC) and thermogravimetric analysis (TGA) can be used to evaluate the thermal stability of the membrane. Detailed information about these technologies can be found in [32,33].

3.2.2. Liquid entry pressure (LEP)

The LEP is defined as the critical transmembrane pressure difference that membrane hydrophobicity could sustain before a larger pressure difference will result in membrane wetting. LEP for the membrane can be approximated from the Laplace equation shown in the Eq. (1):

$$LEP = \Delta P_{inter} = \frac{-2B\gamma_L \cos \theta}{r_{max}} \quad (77)$$

where LEP is liquid entry pressure (Pa).

The liquid/membrane contact angle depends not only on the membrane material but also on the operating temperature and liquid composition. The temperature and composition also influence the liquid surface tension. A correlation of the surface tension of the seawater was reported in [34]:

$$\gamma_L = 77.09 - 0.1788T + 0.0221S \quad (78)$$

where T is temperature (K), S —salinity (‰).

Valid for $273.15 < T < 313.15$ K; $10 < S < 35$ ‰.

It should also be noted that the LEP changes with operation time. Foulants usually form on the membrane and its hydrophobic surface, and the chemical composition and surface of the membrane are likely to change, all resulting in a lower contact angle and LEP.

Exceeding the LEP causes high concentration feed solution to pass through the membrane and thus impair the separation, so high LEP is needed to ensure the product quality.

3.2.3. Membrane permeability (C)

The membrane permeability is defined as the ratio of the mass flux to the vapor pressure difference across the membrane:

$$C = \frac{J}{p_{f,m} - p_{p,m}} \quad (79)$$

where C is membrane permeability ($\text{kg}/(\text{m}^2 \text{ s Pa})$), J —mass flux ($\text{kg}/(\text{m}^2 \text{ s})$), $p_{f,m}$ —vapor pressure at the membrane feed-side surface (Pa), $p_{p,m}$ —vapor pressure at the membrane permeate-side surface (Pa).

C is used to characterize the membrane's ability to produce a mass flux for a given vapor pressure difference. C can be determined from experiments, but mass transport models can also be used as discussed in Section 2.3.

In DCMD, the vapor pressure at the feed and the permeate side of the membrane surface is usually calculated using the saturated pressure of the membrane feed and permeate side surface temperatures. In AGMD, SGMD, and VMD, the vapor pressure at the permeate side of the membrane surface is just the partial pressure of the vapor while the vapor pressure at the feed side of the membrane surface is calculated using the saturated pressure corresponding to the temperature at the membrane feed side surface.

As explained in Section 2.3 about the mass transport mechanisms, the permeability depends on the properties of the membrane and on the operating conditions, such as temperature, total pressure, and the partial pressure of the air and non-condensable gas present in the membrane. The air and other non-condensable gases present in the membrane pores create additional mass transport resistance to the vapor, so generally the mass flux decreases as the partial pressure of the non-condensable gas in the membrane pore increases [35,36].

3.2.4. Mass transport pre-factor (PF)

The “mass transport pre-factor” [37] is used to evaluate the membrane’s mass transport ability based on its major transport-related properties and is defined as:

$$PF = \frac{r^\beta \cdot \varepsilon}{\tau \cdot \delta} \quad (80)$$

where β is exponential factor depends on the mass transport mechanism. For the Knudsen diffusion mechanism, $\beta = 1$; for the viscous flow mechanism, $\beta = 2$; for the ordinary molecular diffusion mechanism, $\beta = 0$. PF —mass transport pre-factor (m^{-1}) for $\beta = 0$, (dimensionless) for $\beta = 1$, (m) for $\beta = 2$, r —average pore radius (m), ε —membrane porosity (dimensionless), τ —membrane tortuosity (dimensionless), δ —membrane thickness (m).

As discussed in Section 2.3, three mass transport mechanisms are generally considered in MD. They can be expressed as follows:

For the Knudsen mechanism:

$$\begin{aligned} J &= \frac{2r\varepsilon}{3\tau\delta} \left(\frac{8M}{\pi RT_{mem}} \right)^{\frac{1}{2}} (p_{f,m} - p_{p,m}) \\ &= PF \times \frac{2}{3} \left(\frac{8M}{\pi RT_{mem}} \right)^{\frac{1}{2}} (p_{f,m} - p_{p,m}) \end{aligned} \quad (81)$$

For the ordinary molecular diffusion mechanism:

$$\begin{aligned} J &= \frac{\varepsilon}{\tau\delta} \frac{DM}{RT_{mem}} \frac{P_{mem}}{p_{air}} (p_{f,m} - p_{p,m}) \\ &= PF \times \frac{DM}{RT} \frac{P_{mem}}{p_{air}} (p_{f,m} - p_{p,m}) \end{aligned} \quad (82)$$

For the viscous flow mechanism:

$$\begin{aligned} J &= \frac{1}{8\mu} \frac{r^2 \varepsilon M P_{mem}}{\tau\delta RT_{mem}} (P_{f,m} - P_{p,m}) \\ &= PF \times \frac{1}{8\mu} \frac{M P_{mem}}{RT_m} (P_{f,m} - P_{p,m}) \end{aligned} \quad (83)$$

It can be seen that in all these mass transport mechanisms, the mass flux is a function of membrane properties and operating conditions. PF is the term representing the effect of membrane properties. However, when more than one mechanism plays an important role in overall mass flux, this method cannot be applied since the relative importance of each mechanism should be considered.

3.2.5. Conduction heat transfer coefficient of the membrane (h_m)

The conduction heat transfer coefficient of the membrane is defined as the ratio of the effective membrane thermal conductivity to the membrane thickness:

$$h_m = \frac{k_m}{\delta} = \frac{\varepsilon k_g + (1 - \varepsilon)k_s}{\delta} \quad (84)$$

where h_m is conduction heat transfer coefficient of the membrane ($\text{W}/(\text{m}^2 \text{K})$), k_m —effective membrane thermal conductivity ($\text{W}/(\text{mK})$), δ —membrane thickness (m), ε —membrane porosity (dimensionless), k_g —thermal conductivity of the gas present in the pores ($\text{W}/(\text{mK})$), k_s —membrane material thermal conductivity ($\text{W}/(\text{mK})$).

As discussed in Section 2.2, the transmembrane conduction heat transfer is considered as a heat loss in the MD process and is proportional to h_m , so h_m influences the energy efficiency of the MD process.

3.3. Production rate criteria

The performance criteria used to evaluate the production rate of MD process are discussed in this section. The product of the MD process can be the

distillate and/or the concentrated feed solution, with the production rate of these two closely related. Since they are the two products of the same process, a higher production rate of the distillate means a higher concentration rate of the feed solution.

3.3.1. Product mass flow rate (\dot{m}_{pro})

The product mass flow rate is defined as the mass production of product per unit time.

$$\dot{m}_{pro} = \frac{dm_{pro}}{dt} \quad (85)$$

where \dot{m}_{pro} is product mass flow rate (kg/s), m —mass production of the product (kg), t —time period (s).

The flow rate of the product is sometimes defined volumetrically (not by mass) \dot{V}_{pro} :

$$\dot{V}_{pro} = \frac{dV_{pro}}{dt} \quad (86)$$

where \dot{V}_{pro} is product volumetric flow rate (m^3/s), V_{pro} —volumetric production of the product (m^3).

The product mass flow rate directly evaluates the production rate of MD process.

3.3.2. Mass flux (J)

The term “mass flux” is used here to denote the flux of the distillate across a membrane, defined as the mass flow rate of the distillate across the membrane per unit membrane area:

$$J = \frac{\dot{m}_d}{A} \quad (87)$$

where J is mass flux ($kg/(m^2 s)$), \dot{m}_d —mass flow rate of the distillate (kg/s), A —membrane area (m^2).

The flux is sometimes defined volumetrically (not by mass) J_v :

$$J_v = \frac{\dot{V}_d}{A} \quad (88)$$

where J_v is volumetric flux (m/s), \dot{V}_d —volumetric flow rate of the distillate (m^3/s).

Mass flux is a widely used performance criterion in MD. Practical long-time use of MD requires additional important performance criteria, led by long-time operational effects (such as fouling and membrane deterioration) on it, energy consumption (such as heat

consumption, electrical energy consumption, and exergy analysis), product quality, and of course cost of unit product.

3.3.3. Relative concentration change rate (CR)

The relative concentration change rate is defined as the time rate of change of the ratio of the solutes (or, rarely, solvent) concentration to the initial concentration:

$$CR = \frac{c(t)}{c_{initial}} \frac{1}{t} = \frac{CF}{t} \quad (89)$$

where CR is relative concentration change rate (s^{-1}), $c(t)$ —concentration of the solvent or solute at time t (mol/m^3), $c_{initial}$ —concentration of the solutes at initial condition (mol/m^3), t —time period (s).

CR is directly related to the mass flux. For a feed solution that contains non-volatile solutes and with a pure distillate, mass conservation requires:

$$CR = \frac{N_{so}/(V_{initial} - \bar{J}_v At)}{N_{so}/V_{initial}} = \frac{V_{initial}}{V_{initial} - \bar{J}_v At} \quad (90)$$

where N_{so} is mole number of the solutes (mol), $V_{initial}$ —initial volume of the solution (m^3), \bar{J}_v —average volumetric flux (m/s).

3.4. Product quality criteria

The performance criteria used to characterize the product quality of MD process are discussed in this section.

3.4.1. Volumetric molar concentration (c)

The volumetric molar concentration is defined as the number of moles of the species divided by the volume of the solution:

$$c = \frac{N}{V} \quad (91)$$

where c is volumetric molar concentration of the species (mol/m^3), N —mole number of the species (mol), V —volume of the solution (m^3).

The mass fraction is also widely used as an alternative criterion of molar concentration. The mass fraction is defined as the mass of the species divided by the mass of the solution:

$$w = \frac{m_{sp}}{m_t} \quad (92)$$

where w is mass fraction of the species (dimensionless), m_{sp} —mass of the species (kg), m_t —mass of the solution (kg).

The mass fraction is often expressed in % or ppm. Specifically, for water desalination application, the mass fraction of solutes in water is called salinity.

The molar concentration or the mass fraction serve as a criterion to evaluate the quality of the distillate and concentrated feed solution. Measurement of the concentration requires chemical analysis, so it is in some cases measured much more simply and quickly by measuring the solution electrical conductivity and using an empirical relation between the solute concentration and that conductivity, which of course depends also on the types of solutes and solution temperature.

3.4.2. Rejection factor (R)

The rejection factor is defined as the ratio of the solutes molar concentration difference between the feed solution and the distillate, to the solutes molar concentration of the feed solution:

$$R = \frac{c_f - c_d}{c_f} \quad (93)$$

where R is rejection factor (dimensionless), c_f —solute molar concentration of the feed solution (mol/m^3), c_d —solute molar concentration of the distillate (mol/m^3).

It is a criterion used to evaluate the quality of the distillate and it modifies the concentration information to a dimensionless ratio.

3.4.3. Concentration factor (CF)

The concentration factor is defined as the ratio of the solutes concentration to the initial concentration:

$$CF = \frac{c}{c_{initial}} \quad (94)$$

where CF is concentration factor (dimensionless), c —molar concentration of the solutes (mol/m^3), $c_{initial}$ —molar concentration of the solutes at initial condition (mol/m^3).

The concentration factor of the feed solution evaluates the extent of the feed solution being concentrated or the volatile solutes being removed from the feed solution.

3.4.4. Separation factor (α)

The separation factor is defined as:

$$\alpha = \frac{x_p/(1-x_p)}{x_f/(1-x_f)} \quad (95)$$

where α is separation factor (dimensionless), x_p —mole fraction of the desired component in the permeate stream (dimensionless), x_f —mole fraction of the desired component in the feed stream (dimensionless).

Though most of the MD applications deal with non-volatile solutes, some studies use MD to separate aqueous solution containing volatile organic compounds [38–42]. For these applications, the separation factor provides an evaluation of the concentration difference between the feed component of interest and the permeate streams, thus evaluating the ability of MD to separate that component.

3.5. Energy performance criteria

Most of the energy performance criteria evaluate the energy efficiency of the MD on the system level, which includes not only the membrane module but also other components needed for the overall operation of the MD process. For an MD system shown in Fig. 8, the control volume of this system is outlined by the dashed line in Fig. 14.

3.5.1. Specific heat consumption (SHC)

The specific heat consumption is defined as the amount of heat supplied to produce a unit mass of the product. This performance criterion is used to evaluate the heat utilization performance of the MD on the system level (Fig. 14).

$$SHC_m = \frac{\dot{Q}_{in}}{\dot{m}_{pro}} \quad (96)$$

where SHC_m is specific heat consumption per unit mass of the product (J/kg), \dot{Q}_{in} —total heat input rate (W), \dot{m}_{pro} —mass flow rate of the product (kg/s).

It can also be expressed as the amount of heat supplied to produce a unit volume of the product.

$$SHC_v = \frac{\dot{Q}_{in}}{\dot{V}_{pro}} \quad (97)$$

where SHC_v is specific heat consumption per unit volume of the product (J/m^3), \dot{V}_{pro} —volumetric flow rate of the product (m^3/s).

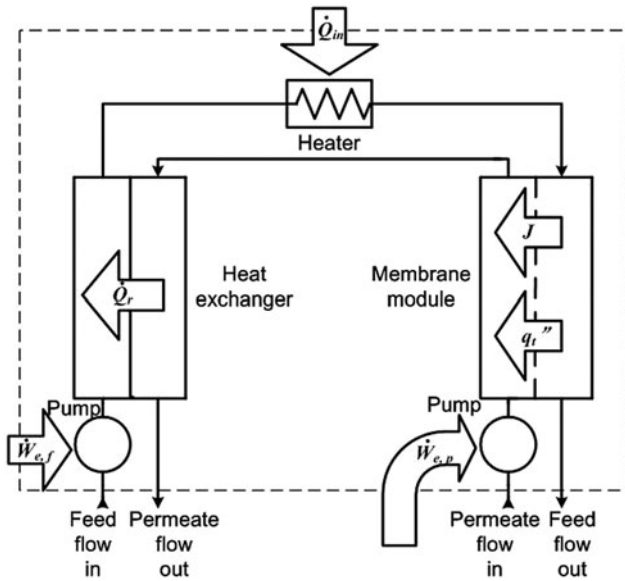


Fig. 14. Schematic of the control volume of a MD system.

SHC evaluates how well the MD heat input is utilized to produce the desired product on the system level.

3.5.2. Specific electrical energy consumption (SEEC)

The specific electrical energy consumption is defined as the amount of electrical energy supplied to produce a unit mass of the product. This performance criterion is used to evaluate the electrical energy performance of the MD on the system level (Fig. 14):

$$SEEC_m = \frac{\dot{W}_{e,in}}{\dot{m}_{pro}} \quad (98)$$

where $SEEC_m$ is specific electrical energy consumption per unit mass of the product (J/kg), $\dot{W}_{e,in}$ —total electrical energy input rate (W), \dot{m}_{pro} —mass flow rate of the product (kg/s).

It can also be expressed as the amount of electrical energy supplied to produce a unit volume of the product.

$$SEEC_V = \frac{\dot{W}_{e,in}}{\dot{V}_{pro}} \quad (99)$$

where $SEEC_V$ is specific electrical energy consumption per unit volume of the product (J/m³), \dot{V}_{pro} —volumetric flow rate of the product (m³/s).

Consider now the MD system shown by Fig. 14, where the total electrical energy input ($\dot{W}_{e,in}$) is the sum of electrical energy input of the feed flow pump ($\dot{W}_{e,f}$) and the permeate flow pump ($\dot{W}_{e,p}$). As discussed in Sections 2.5 and 2.6, though MD is a thermally driven distillation process, electrical energy is still needed to accomplish tasks such as to drive the feed and the distillate streams, to maintain vacuum in VMD, to drive gas stream in SGMD and run auxiliaries including pre- and post-treatment for the operation of the whole system. Also, since heat and electrical energy have different thermodynamic quality and they generally come from different source, it is necessary to use a criterion to properly evaluate the electrical energy consumption and other criteria that combined thermal and electrical energy consumption in MD processes.

3.5.3. Membrane thermal efficiency (η)

The membrane thermal efficiency is defined as the ratio of the heat flux by distillate evaporation to total heat flux across the membrane.

$$\eta = \frac{q''_v}{q''_t} = \frac{q''_v}{q''_v + q''_c} = \frac{J\Delta H_{fg}}{J\Delta H_{fg} + h_m(T_{f,m} - T_{p,m})} \quad (100)$$

where η is membrane thermal efficiency (dimensionless), q''_v —heat flux across the membrane by evaporation (W/m²), q''_c —heat flux across the membrane by conduction (W/m²), q''_t —total heat flux across the membrane (W/m²), ΔH_{fg} —specific enthalpy of vaporization (J/kg), h_m —conduction heat transfer coefficient of the membrane (W/(m² K)), $T_{f,m}$ —temperature at the membrane feed-side surface (K), $T_{p,m}$ —temperature at the membrane permeate-side surface (K).

As discussed in Section 2.2, q''_v is the heat exclusively used for production of the distillate, and the sensible heat transferred q''_c is regarded as an energy loss, so the membrane thermal efficiency evaluates the heat utilization efficiency for distillation of the heat transport process across membrane (A in Fig. 15). It should be noticed that, as shown in Sections 2.2 and 2.3, the membrane thermal efficiency depends on not only the membrane properties, but also the operation conditions and module configurations. Also, if the energy losses to the environment are neglected, it can also be used to evaluate the heat utilization efficiency of the membrane module (B in Fig. 15), since the heat transfer across the membrane is the only energy interaction between the feed and the permeate stream.

An important issue is that some energy performance criteria like membrane thermal efficiency focus

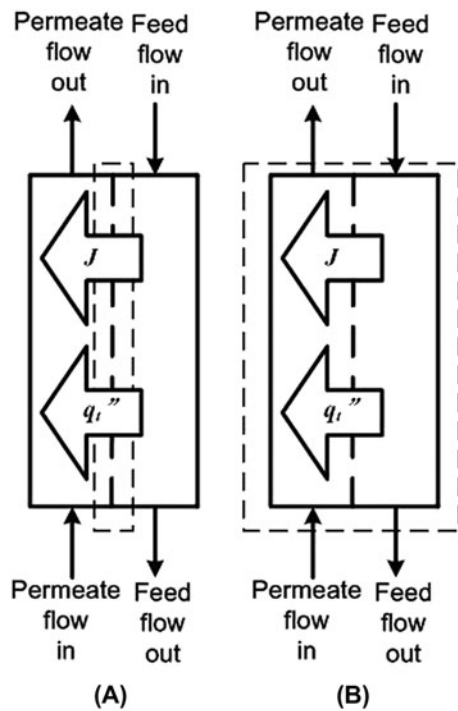


Fig. 15. Schematic of the control volume of the membrane (dashed line in A) and the membrane module (dashed line in B).

only on a single system component or aspect, most notably the membrane transport, but a plant typically includes many other auxiliary energy-consuming units as discussed in Section 2.5. Unless such units have negligible impact on overall plant energy performance, they must be included in calculating its energy performance, which also requires the definition of an overall energy performance criterion. Also, the overall energy consumption depends on the use of the heat recovery devices which cannot be revealed by this membrane thermal efficiency.

3.5.4. Gain output ratio (GOR)

The gain output ratio (GOR) in MD is usually defined as the ratio of the transmembrane heat transfer rate by the distillate evaporation for the generation of the distillate, to the heat input rate. This performance criterion is used to evaluate the heat utilization performance of the MD on the system level (Fig. 14).

GOR is a criterion widely used to evaluate the heat utilization efficiency of thermal desalination system including MD. For the desalination process in which the heat input is by externally supplied steam that gives its heat by condensation, it is typically used as the second term on the right-hand side of Eq. (101)

indicates. However, this term is correct only when the heat supplied by externally delivered condensing steam and its condensate, and the vapor flow across the membrane, are all saturated without sensible heat change. A more general definition of the second term on the right-hand side is given in Eq. (102):

$$GOR = \frac{q_v'' A}{\dot{Q}_{in}} = \frac{\dot{m}_d \Delta H_{fg,d}}{\dot{m}_s \Delta H_{fg,s}} \quad (101)$$

where GOR is gain output ratio (dimensionless), q_v'' —heat flux across the membrane by evaporation (W/m^2), A —membrane area (m^2), \dot{Q}_{in} —heat input rate (W), \dot{m}_d —mass flow rate of the distillate (kg/s), \dot{m}_s —mass flow rate of the input steam (kg/s), $\Delta H_{fg,d}$ —specific enthalpy of vaporization for the distillate (J/kg), $\Delta H_{fg,s}$ —specific enthalpy of vaporization for the steam (J/kg).

A fundamental constraint of defining GOR by the second term on the right-hand side of Eq. (101) is that expression of the ratio between the heat quantities needed for producing a mass flow rate \dot{m}_d of distilled product, and the heat provided by the mass flow rate \dot{m}_s of the input steam, must take into account that: (a) neither the distillation heat demand, nor the steam heat supply are performed exactly at the saturation conditions at practical plant conditions: the produced distillate vapor is typically superheated and is therefore first cooled to the saturation point before it is condensed, consequently demanding this sensible heat of cooling, and the distillate condensate is typically somewhat supercooled, consequently demanding also the sensible heat of subcooling, and these amounts of heat should then be added to the latent heat of evaporation of the feed solution. The heat supplied by the steam input similarly has the sensible heat components of superheat and subcooling, and (b) the feed solution enthalpy and latent heats of evaporation and condensation depend on the evaporation temperature and pressure of the feed solution that, in turn, depend on solution composition and concentrations, and on the plant design. A correct definition is given in Eq. (102).

$$GOR = \frac{q_v'' A}{\dot{Q}_{in}} = \frac{\dot{m}_d [(H_{d,i} - H_{d,sat}) + \Delta H_{fg,d} + (H_{d,sat} - H_{d,o})]}{\dot{m}_s [(H_{s,i} - H_{s,sat}) + \Delta H_{fg,s} + (H_{s,sat} - H_{s,o})]} \quad (102)$$

where $H_{d,i}$ is specific enthalpy of the superheated distillate (J/kg), $H_{d,sat}$ —specific enthalpy of the saturated

distillate (J/kg), $H_{d,o}$ —specific enthalpy of the supercooled distillate (J/kg), $H_{s,i}$ —specific enthalpy of the superheated steam (J/kg), $H_{s,sat}$ —specific enthalpy of the saturated steam (J/kg), $H_{s,o}$ —specific enthalpy of the supercooled steam (J/kg).

GOR is a criterion for how well the heat input is utilized to produce distillate on the system level. For MD systems in which the product is the distillate, GOR is directly related to SHC:

$$GOR = \frac{(H_{d,i} - H_{d,sat}) + \Delta H_{fg,d} + (H_{d,sat} - H_{d,o})}{SHC_m} \quad (103)$$

Besides the above-discussed constraints, the definition of any performance criterion that is based on heat only is incomplete and could be very misleading if the amount of associated work input is not negligible relative to the associated amounts of heat. As one extreme example in which a criterion based on heat only is completely correct, is when only heat is used where even the pumping is, say, buoyancy driven, and the system does not use any mechanically or electrically driven pumps. The other extreme is where no heat is used and all the energy input/output is by mechanical work, such as in RO processes. An intermediated example are various thermal distillation processes including MD where the dominant energy is heat but work for pumping is not negligible relative to it.

3.5.5. Heat recovery factor (H_r)

The heat recovery factor is defined as the ratio of the heat rate recovery (rate of heat gain by the feed stream in the heat recovery device as shown in Fig. 8 and can be calculated by Eq. (52)) for reuse in the process, to the total heat transfer rate across the membrane. We have chosen this denominator because it represents the fundamentally maximal amount of heat that can be recovered. This performance criterion is used to evaluate the heat utilization performance of the MD on the system level (Fig. 14).

$$H_r = \frac{\dot{Q}_r}{q''_t A} \quad (104)$$

where H_r is heat recovery factor (dimensionless), \dot{Q}_r —heat recovery rate (W), q''_t —heat flux across the membrane by evaporation (W/m²), A —membrane area (m²).

H_r evaluates the internal heat recovery extent in the MD system. A higher H_r means more heat is recovered and less heat input is needed, thus a higher

heat utilization efficiency of the system is achieved. It is noteworthy that increase of the heat recovery factor requires a more complex system and raises other energy consumption such as pump work. Furthermore, since heat recovery is typically implemented by employing multi-stage operation, the driving forces (temperature and pressure differences) in each stage are proportionally lowered, resulting in lower product mass fluxes in each stage.

3.5.6. Performance ratio (PR)

Rooted in the past overwhelming use of thermal distillation, for which the needed heat was supplied in most cases by steam from boilers or back-pressure steam turbines, this widely used PR is defined as the ratio of the mass flow rate of the produced distillate to the mass flow rate of the input steam used to generate the distillate. In MD the heat input is typically not steam, so the \dot{Q}_{in} appeared in the Eq. (102) needs to be modified to the equivalent weight of steam to calculate PR. This performance criterion is used to evaluate the heat utilization performance of the MD on the system level (Fig. 14).

$$PR = \frac{\dot{m}_d}{\dot{m}_s} \quad (105)$$

where PR is performance ratio (dimensionless), \dot{m}_d —mass flow rate of the distillate (kg/s), \dot{m}_s —mass flow rate of the input steam (kg/s).

While this definition is very practical because it is easy to measure and also reflects a partially relevant income-to-energy expense economic ratio, it does not represent correctly an energy ratio like the GOR (Eq. (102)) and lacks scientific generality. Further comments are shown in the above discussion of the GOR.

Since the latent heat of evaporation for the distillate is almost the same as the condensation latent heat of the heating steam, PR can be regarded as an approximation of GOR without considering the sensible heat change in the process which expressed in the ratio of mass flow rate.

Since PR and GOR evaluate the same characteristics of the process, PR has the same advantages and limitations mentioned in the discussion of GOR.

3.5.7. Flow pressure drop (ΔP)

This is a ubiquitous criterion, defined as the pressure change of a flow stream from a defined inlet to a defined outlet:

$$\Delta P = P_{in} - P_{out} \quad (106)$$

where ΔP is flow pressure drop (Pa), P_{in} —flow pressure at the defined flow inlet (Pa), P_{out} —flow pressure at the defined flow outlet (Pa).

ΔP is an important criterion for all processes involving fluid flow including MD. One role is to determine pumping work (proportionally affecting system energy efficiency) and pressure, as well as module and entire system design parameters such as flow cross sections of conduits and their needed strength to withstand the pressures. Another role is in determining distillate transport thermodynamics including vapor transport rate, such as between MSF stages or across MD membranes.

In MD, the membranes are thin, can be mechanically breached if excessive pressure is applied across them, and must be supported by a sufficiently strong backing mesh that consequently also reduces the membrane effective transport area and even promotes fouling. Excessive pressure drop across the hydrophobic membrane will also result in membrane wetting and impairment of the distillate quality, as well as membrane compacting that reduces the mass transport across it.

In typical DCMD and SGMD modules with a counter-flow arrangement, the feed stream pressure decreases along the flow path while the pressure at other side across the membrane increases, so the maximal pressure difference occurs at the inlet or outlet of the feed stream. For AGMD and VMD modules, the feed stream pressure decreases along the flow path while pressure is constant at other side across the membrane, so maximum pressure difference arises at inlet of the feed stream.

3.5.8. Fuel energy saving ratio (FESR)

As described in Section 2.5, properly designed dual- or multi-purpose desalination plants use less energy as compared with separate power-only and water-only systems with same loads of outputs, and the fuel energy saving ratio [23] is used to evaluate the energy saving performance of multi-purpose desalination plants. The fuel energy saving ratio is defined as the ratio of heat consumption saving by using the multi-purpose desalination plant compared with using separate reference single-purpose-only systems having the same outputs as the multi-purpose plant, to the total heat consumption of these separate reference systems. Most common is the dual purpose,

water and power plants, and its FESR, applying at the system level (Fig. 9) is:

$$FESR = \frac{\dot{Q}_{pow} + \dot{Q}_{wat} - \dot{Q}_{dual}}{\dot{Q}_{pow} + \dot{Q}_{wat}} \quad (107)$$

where FESR is fuel energy saving ratio (dimensionless), \dot{Q}_{pow} —heat consumption rate of the reference power-only system with same electrical energy output rate as the dual-purpose desalination system (W), \dot{Q}_{wat} —heat consumption rate of the reference water-only system with same water production rate as the dual-purpose desalination system (W), \dot{Q}_{dual} —heat consumption rate of the dual-purpose desalination plant (W).

For such a dual-purpose desalination system with electrical energy generation rate $\dot{W}_{e,dual}$ and water production rate $\dot{m}_{d,dual}$, \dot{Q}_{pow} can be calculated by:

$$\dot{Q}_{pow} = \frac{\dot{W}_{e,dual}}{\eta_{e,ref}} \quad (108)$$

where $\dot{W}_{e,dual}$ is electrical energy production rate of the dual-purpose desalination plant (W), $\eta_{e,ref}$ —heat to electrical energy conversion factor for the reference power plant (dimensionless).

Similarly, \dot{Q}_{wat} is calculated by:

$$\dot{Q}_{wat} = \frac{\dot{m}_{d,dual}}{\eta_{w,ref}} \quad (109)$$

where $\dot{m}_{d,dual}$ is water production rate of the dual-purpose desalination plant (kg/s), $\eta_{w,ref}$ —heat to water conversion factor for the reference desalination plant (kg/J).

This criterion can also be modified in the similar manner to evaluate the energy saving performance for MD coupled with other processes.

$$FESR = \frac{\dot{Q}_{oth} + \dot{Q}_{MD} - \dot{Q}_{coup}}{\dot{Q}_{oth} + \dot{Q}_{MD}} \quad (110)$$

where \dot{Q}_{oth} is heat consumption rate of the reference system performs only the “other process” with same output rate of the other product as the couple system (W), \dot{Q}_{MD} —heat consumption rate of the reference MD system with the same product output rate as the coupled system (W), \dot{Q}_{coup} —heat consumption rate of the coupled system (W).

3.5.9. Specific equivalent electrical energy consumption (EEEC)

For dual-purpose desalination plants, the specific equivalent electrical energy consumption is defined as the ratio of the reduction of the electrical energy production of the dual-purpose desalination plant compared with the reference power-only system for the same total heat input, to the mass flow rate of the water produced by the dual-purpose desalination plant. This performance criterion can be used to evaluate the energy performance of a dual-purpose MD plant at the system level (Fig. 9).

$$EEEC_m = \frac{\dot{W}_{e,ref} - \dot{W}_{e,dual}}{\dot{m}_{d,dual}} = \frac{\dot{Q}_{in}(\eta_{e,ref} - \eta_{e,dual})}{\dot{m}_{d,dual}} \quad (111)$$

where $EEEC_m$ is specific equivalent electrical energy consumption per unit mass of the product (J/kg), $\dot{W}_{e,ref}$ —electrical energy output rate of the reference power-only system with the same total heat input as the dual-purpose desalination plant (W), $\dot{W}_{e,dual}$ —electrical energy output rate of the dual-purpose desalination plant (W), $\dot{m}_{d,dual}$ —water production rate of the dual-purpose desalination plant (kg/s), \dot{Q}_{in} —total heat input rate (W), $\eta_{e,ref}$ —heat to electrical energy conversion factor for the reference power plant (dimensionless), $\eta_{e,dual}$ —heat to electrical energy conversion factor for the dual-purpose desalination plant (dimensionless).

It can also be expressed based on the volume of the water produced.

$$EEEC_V = \frac{\dot{W}_{e,ref} - \dot{W}_{e,dual}}{\dot{V}_{d,dual}} = \frac{\dot{Q}_{in}(\eta_{e,ref} - \eta_{e,dual})}{\dot{V}_{d,dual}} \quad (112)$$

where $EEEC_V$ is specific equivalent electrical energy consumption per unit volume of the product (J/m³), $\dot{V}_{d,dual}$ —volumetric water production rate (m³/s).

Though a dual-purpose desalination plant saves energy compared with separate power-only and water-only systems, it produces less electrical energy compared with power-only system with same amount of heat input. The production of the water is thus at the expense of this electrical energy reduction and the $EEEC$ evaluates this equivalent electrical energy consumption of the dual-purpose desalination plant. This criterion provides a metric to compare the heat utilization efficiency of the dual-purpose desalination plant to the separate power-only and water-only systems.

3.6. Exergy performance criteria

Definitions of the various forms of exergy efficiency are available in many publications (e.g. [43,44]) and are summarized in [45]. Those most applicable to MD follow.

Exergy analyses have been conducted for MD processes [46–48], but various different expressions are used in different papers to calculate the exergy and most of them are based on significant simplifications. Comparisons and clarifications of some of these expressions are in [15]. The general expressions for exergy are discussed in Section 2.6.

3.6.1. Overall exergy efficiency (ψ_t)

The overall exergy efficiency is defined as the ratio of the exergy output to the exergy input for the control volume of interest. This performance criterion is used to evaluate the exergy performance of MD on the system level (Fig. 14), or of a specific component of the system (such as the membrane module (B in Fig. 15)).

$$\psi_t = \frac{\dot{E}_{output}}{\dot{E}_{input}} = 1 - \frac{\dot{E}_{des}}{\dot{E}_{input}} \quad (113)$$

where ψ_t is overall exergy efficiency (dimensionless), \dot{E}_{input} —exergy input rate (W), \dot{E}_{output} —exergy output rate (W), \dot{E}_{des} —exergy destruction rate (W).

The calculation of the exergy input and output of a simple MD system are discussed in Section 2.6. This criterion can also be used to analysis the subprocess within the system which often takes place in a single component (such as the membrane module (B in Fig. 15)).

Overall exergy efficiency evaluates the effectiveness of the energy use and the irreversibility in the process. It is especially useful if there is intent to use the exergy potential of output streams and energy outputs other than that of the intended separation product. This also leads to its limitation: it does not focus on the typically most wanted separation (e.g. desalination) system product (e.g. the desalted water), but includes all system outputs, most of which are usually not useful; furthermore, although they are an integral part of the selected process, most of them are undesirable for practical purposes, since they are wastes such as hot concentrated brines that contain various additives such as anti-foaming and anti-scaling chemicals, etc., heat emissions, streams with kinetic energy that disturb the biota, etc., which have negative environmental and economic impacts.

3.6.2. Utilitarian exergy efficiency (ψ_u)

The utilitarian exergy efficiency of a chosen control volume is defined as the ratio of the exergy output useful to the owner, to the exergy input paid by the owner. This performance criterion is used to evaluate the exergy performance of the MD on the system level (Fig. 14), or of a specific component of the system (such as the membrane module (B in Fig. 15)).

$$\psi_u = \frac{\dot{E}_u}{\dot{E}_p} \quad (114)$$

where ψ_u is utilitarian exergy efficiency (dimensionless), \dot{E}_u —paid exergy input rate (W), \dot{E}_p —useful exergy output rate (W).

The paid and useful exergies are defined depending on the need of the user, and thus somewhat arbitrarily. For the MD process in which we focus on the product (distillate and/or concentrated feed solution) of the separation, the useful exergy output can be taken as the exergy contained in the product, and ψ_u thus becomes:

$$\psi_u = \frac{\dot{E}_{pro}}{\dot{E}_p} \quad (115)$$

where \dot{E}_{pro} is product exergy output rate (W).

It should be noted that this product (in Eq. (115)) may be not only the desired product that is valuable to the user, but also the undesired product which the user must remediate.

For the paid exergy, consider a simple DCMD, AGMD, SGMD, VMD system as Figs. 10–13 show. Generally, the paid exergy input of these systems includes exergy of the electrical energy consumption of the electrical devices such as pumps and blowers ($\dot{W}_{e,f}$, $\dot{W}_{e,p}$, $\dot{W}_{e,b}$, $\dot{W}_{e,b}$, $\dot{W}_{e,v}$) and the exergy of the heat consumption of the heater (\dot{Q}_{in}).

Compared with overall exergy efficiency ψ_t , the utilitarian exergy efficiency ψ_u , is more oriented to the desire of the user to evaluate the potential economic value of the process and for guidance for economic system improvement.

3.6.3. Specific exergy consumption (SXC)

The specific exergy consumption is defined as the amount of exergy supplied to produce a unit mass of the product. This performance criterion is used to evaluate the exergy performance of the MD on the system level (Fig. 14).

$$SXC_m = \frac{\dot{E}_{input}}{\dot{m}_{pro}} \quad (116)$$

where SXC_m is specific exergy consumption per unit mass of the product (J/kg), \dot{E}_{input} —total exergy input rate (W), \dot{m}_{pro} —mass flow rate of the product (kg/s).

It can also be expressed as the amount of exergy supplied to produce a unit volume of the product.

$$SXC_V = \frac{\dot{E}_{input}}{\dot{V}_{pro}} \quad (117)$$

where SXC_V is specific exergy consumption per unit volume of the product (J/m³), \dot{V}_{pro} —volumetric flow rate of the product (m³/s).

SXC evaluates how well the exergy input is used to produce the product. It provides a metric to combine the thermal and electrical energy consumption in MD based on the second law of thermodynamics.

3.6.4. Exergy consumption ratio (XCR)

The exergy consumption ratio is defined as the ratio of the minimal specific exergy consumption needed for the separation (SXC_{min}) to the specific exergy consumption of the system (SXC). This performance criterion is used to evaluate the exergy performance of the MD on the system level (Fig. 14).

$$XCR = \frac{SXC_{min}}{SXC} \quad (118)$$

where XCR is exergy consumption ratio (dimensionless), SXC_{min} —minimal specific exergy consumption per unit mass of the product (J/kg), SXC—specific exergy consumption per unit mass of the product (J/kg).

SXC_{min} (which is same the minimum work of separation (W_{min})) can be calculated from the separation exergy needed for a thermodynamically reversible separation process. Since the exergy destruction equals to 0 in a reversible process, the exergy balance (Eq. (65)) yields:

$$\dot{m}_{pro}SXC_{min} + \dot{E}_{flow,f} = \dot{E}_{flow,d} + \dot{E}_{flow,cf} \quad (119)$$

where \dot{m}_{pro} is mass flow rate of the product (kg/s), $\dot{E}_{flow,f}$ —flow exergy of the inlet feed solution (W), $\dot{E}_{flow,d}$ —flow exergy of the distillate (W), $\dot{E}_{flow,cf}$ —flow exergy of the concentrated feed solution (W).

According to Eq. (119), SXC_{min} can be calculated by:

$$SXC_{min} = W_{min} = \frac{\dot{E}_{flow,d} + \dot{E}_{flow,cf} - \dot{E}_{flow,f}}{\dot{m}_{pro}} \quad (120)$$

where W_{min} is minimal work of separation (J/kg).

The calculation of the flow exergy is discussed in Section 2.6. A detail calculation of the SXC_{min} for the saline water can be found in [21].

SXC evaluates how well the exergy input is utilized to produce product and the extent to which the practical MD separation process approaches the ideal reversible process.

3.6.5. Multi-purpose plant exergy saving ratio (XSR)

For multi-purpose desalination plants, the exergy saving ratio can be defined as the ratio of the exergy consumption saved by using the multi-purpose desalination plant compared with using separate reference single-purpose-only systems having the same outputs as the multi-purpose plant, to the total exergy consumption of these separate reference single-purpose-only systems. This performance criterion can be used to evaluate the exergy performance of such an MD plant at the system level (Fig. 9), and is defined for the most commonly used type, the water production and power generation one, by:

$$XSR = \frac{\dot{E}_{pow} + \dot{E}_{wat} - \dot{E}_{dual}}{\dot{E}_{pow} + \dot{E}_{wat}} \quad (121)$$

where XSR is exergy saving ratio (dimensionless), \dot{E}_{pow} —exergy consumption rate of the reference power-only plant with the same electrical energy output rate as the dual-purpose desalination plant (W), \dot{E}_{wat} —exergy consumption rate of the reference water-only plant with the same water production rate as the dual-purpose desalination plant (W), \dot{E}_{dual} —exergy consumption rate of the dual-purpose desalination plant (W).

Considering a dual-purpose desalination system whose exergy consumption rate is \dot{E}_{dual} , having an electrical energy production rate $\dot{W}_{e,dual}$ and desalted water production rate $\dot{m}_{d,dual}$. \dot{E}_{pow} can be calculated by:

$$\dot{E}_{pow} = \frac{\dot{W}_{e,dual}}{\zeta_{e,ref}} \quad (122)$$

where $\dot{W}_{e,dual}$ is electrical energy production rate of the dual-purpose desalination plant (W), $\zeta_{e,ref}$ —exergy

to electrical energy conversion factor for the reference power plant (dimensionless).

Similarly, \dot{E}_{wat} is calculated by:

$$\dot{E}_{wat} = \frac{\dot{m}_{d,dual}}{\zeta_{w,ref}} \quad (123)$$

where $\dot{m}_{d,dual}$ is water production rate of the dual-purpose desalination plant (W), $\zeta_{w,ref}$ —exergy to water conversion factor for the reference desalination plant (kg/J).

This criterion is used to evaluate the exergy saving performance of the dual-purpose desalination plants. It can also be modified in a similar manner to evaluate the exergy saving performance for MD coupled with other processes.

$$XSR = \frac{\dot{E}_{oth} + \dot{E}_{MD} - \dot{E}_{coup}}{\dot{E}_{oth} + \dot{E}_{MD}} \quad (124)$$

where \dot{E}_{oth} is exergy consumption rate of the reference system that performs only the “other process” with the same product output rate as the coupled system (W), \dot{E}_{MD} —exergy consumption rate of the reference MD system with same product output rate as the coupled system (W), \dot{E}_{coup} —exergy consumption rate of the coupled system (W).

3.6.6. Relative exergy destruction ratio (XDR)

The relative exergy destruction ratio is defined as the ratio of the exergy destruction in a subsystem or subprocess (e.g. taking place in one of the system components) to the total exergy input of the system.

$$XDR = \frac{\dot{E}_{des,sub}}{\dot{E}_{input}} \quad (125)$$

where XDR is relative exergy destruction ratio (dimensionless), $\dot{E}_{des,sub}$ —exergy destruction in the subsystem or subprocess (W), \dot{E}_{input} —total exergy input of the system (W).

Since the total exergy destruction of the system equals to the sum of the exergy destructions of each of its subsystems, the overall exergy efficiency (ψ_t) (Eq. (113)) and XDR are:

$$\sum_j XDR_j = 1 - \psi_t \quad (126)$$

where XDR_j is relative exergy destruction ratio of the subsystem or subprocess j (dimensionless), ψ_t —overall exergy efficiency (dimensionless).

XDR evaluates the extent of the exergy destruction within a subsystem and its thermodynamic performance. Knowledge of the exergy destruction share of the system components gives guidance about the benefits of improving each of them. Detailed exergy analysis of coupled MD systems can be found in [47,48].

3.6.7. Example of calculation of the energy and exergy criteria

While energy analysis is common knowledge, exergy analysis and the comparison between them is less so, and a simple but explicit analysis and calculation example is therefore shown here. The example is based on data from the paper by Banat et al. [48] that shows an exergy analysis of a solar-powered membrane distillation system for 3,000 ppm brackish water. The system was designed and tested to generate process parameters and design data for larger MD system. Our analysis is based on their data collected on 12 June 2006, at 13:00 pm.

In the example we show the method and results for calculating most of the energy and exergy performance parameters and the properties needed for their determination. Not all are necessary for each analysis, and readers can of course select those they need.

Fig. 16 shows the system flow sheet on which our exergy analysis is based. The system consists of three subsystems: a solar collector with a 6 m² solar collection area to provide the heat for the MD process, a PV module with a 0.86 m² area to provide the electricity for driving the MD process pump, and the MD module for desalting the brackish water feed. All of the input energy is thus solar radiation. Since the paper [48] did not present complete data about the PV module, pump and related pressure change, we added these data based on the given related information and sound technical assumptions.

The MD process described in [48] is Permeate Gap Membrane Distillation (PGMD), a version of AGMD where the air gap is removed and the coolant fluid is the feed solution itself. The process flow diagram is shown in Fig. 17. The saline cold feed stream first enters the distillate vapor condenser channel to condense the vapor and at the same time gets pre-heated by the latent heat released by the condensing vapor. Then this pre-heated feed stream enters the heater (here the solar collector) to raise its temperature to the level needed for the MD process, after which it enters the MD evaporator. The preheat process in the

condenser constitutes internal heat recovery and thus a reduction of heat demand by the process. No backup heat or thermal storage was used.

The properties of the fluid at each state point in Fig. 16 are reported in [48] and summarized in Table 1. Since the pressures in the system were not reported, we calculated them as explained in the below-presented discussion about the PV module and pump, with the assumption that 35% of the total pressure drop is incurred from state 1 to 2 and from state 5 to 6, each, and the remaining 30% of the total pressure drop is incurred from state 3 to 4.

The method used to calculate the flow exergy in [48] is replaced here by the method proposed in [49], using Eqs. (58), (59), (61) and thermodynamic property correlations for sea water [34], which applies to the salinity range in this example. The dead state is chosen to be the condition of the feed solution input (state 0) at its ambient conditions, $T_0 = 308.15$ K, $p_0 = 101.325$ kPa, and $w_{s,0} = 3,000$ ppm. The flow enthalpy is calculated by:

$$\dot{H}_i = \dot{m}_i H_i \quad (127)$$

where \dot{H}_i is flow enthalpy of stream i (kW), \dot{m}_i —mass flow rate of stream i (kg/s), H_i —specific enthalpy of stream i (kJ/kg).

Similarly, the flow exergy is calculated by:

$$\dot{E}_i = \dot{m}_i e_i \quad (128)$$

where \dot{E}_i is flow exergy of stream i (kW), e_i —specific flow exergy of stream i (kJ/kg).

Our calculation results are summarized in Table 1.

The performance of the solar collector is also reported in [48] and varies with time due to the variation in solar irradiation intensity and ambient temperature. The solar intensity (I) here was 970 W/m² on 12 June 2006, at 13:00 pm.

The energy efficiency of the solar collector is defined as the ratio of the heat gain by the fluid to the total energy of the solar irradiation.

$$\eta_{sc} = \frac{\dot{H}_4 - \dot{H}_3}{IA_{sc}} \quad (129)$$

where η_{sc} is energy efficiency of the solar collector (dimensionless), \dot{H}_4 —enthalpy of the collector outlet stream, state 4 (W), \dot{H}_3 —enthalpy of the collector inlet stream, state 3 (W), I —solar irradiation (W/m²), A_{sc} —absorption area of the solar collector (m²).

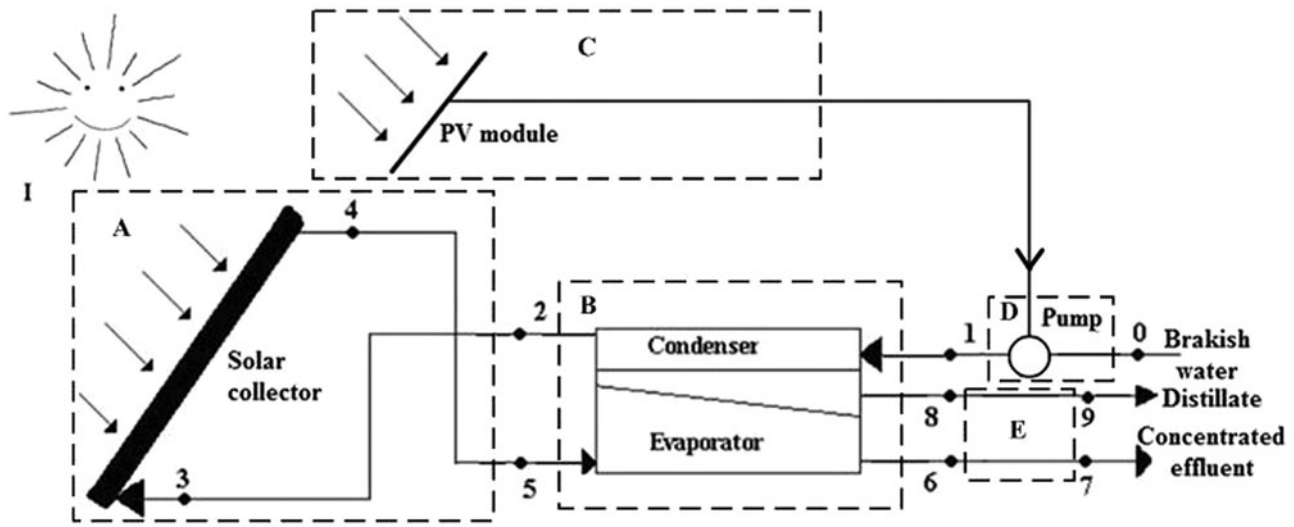


Fig. 16. Schematic of the solar-powered membrane distillation system [48]. The dashed-line boxes enclose the system subprocesses: (A) solar collector subprocess, (B) MD separation subprocess, (C) PV module subprocess, (D) pump subprocess, and (E) discharge subprocess.

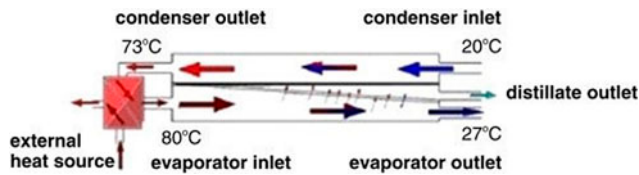


Fig. 17. Module channel arrangement for PGMD [57].

The exergy efficiency of the solar collector is defined as the ratio of the exergy gain by the collector-heated fluid to the total exergy of the solar irradiation.

$$\psi_{sc} = \frac{\dot{E}_4 - \dot{E}_3}{\dot{E}_{sun}} = \frac{\dot{E}_4 - \dot{E}_3}{\dot{e}_{sun} A_{sc}} \quad (130)$$

where ψ_{sc} is exergy efficiency of the solar collector (dimensionless), \dot{E}_4 —low exergy at the collector outlet, state 4 (W).

For the PV module, the energy efficiency is defined here as the ratio of the electrical power generated by this 0.86 m² PV panel to the total energy of the solar irradiation,

$$\eta_{PV} = \frac{\dot{W}_e}{I A_{PV}} = \frac{\dot{w}_e}{I} \quad (131)$$

where η_{PV} is energy efficiency of the PV module (dimensionless), \dot{W}_e —electrical power generated by

the PV module (W), I —solar irradiation (W/m²), A_{PV} —absorption area of the PV panel (m²), \dot{w}_e —electrical power generated by the PV module per unit area (W/m²).

The exergy efficiency of the PV module is defined as the ratio of the electrical power generated by the PV panel to the total exergy of the solar irradiation:

$$\psi_{PV} = \frac{\dot{W}_e}{\dot{E}_{sun}} = \frac{\dot{w}_e}{\dot{e}_{sun}} \quad (132)$$

where ψ_{PV} is exergy efficiency of the solar collector (dimensionless), \dot{W}_e —electrical power generated by the PV module (W), \dot{E}_{sun} —exergy of the solar irradiation (W), \dot{w}_e —electrical power generated by the PV module per unit area (W/m²), \dot{e}_{sun} —exergy of the solar irradiation per unit area (W/m²).

To conduct the energy and exergy analyses, a typical energy efficiency (η_{PV}) of 17.5% is assumed for the PV module, thus 145.5 W electrical power is generated. All the electrical energy is assumed to drive the pump. This small pump's efficiency is assumed to be 12%. Eq. (133) is used with this data to calculate the liquid pressure at state 1, found to be 237.0 kPa, by:

$$\Delta P = \frac{\rho \dot{W}_e \eta_{pump}}{\dot{m}} \quad (133)$$

where ΔP is pressure increase of the fluid in the pump (Pa), \dot{W}_e —electrical power supplied to the pump (W),

Table 1
Properties of the liquids at the various locations in the system

Stream	Temperature, T (K)	Salinity, S (ppm)	Pressure, P (kPa)	Mass flow rate, \dot{m} (kg/min)	Specific enthalpy, H (kJ/kg)	Specific entropy, s (kJ/kg)	Specific chemical potential of water, μ_w (kJ/kg)	Specific chemical potential of salts, μ_s (kJ/kg)	Specific flow exergy, e (kJ/kg)	Flow enthalpy, \dot{H} (kW)	Flow exergy, \dot{E} (W)
0	308.15	3,000	101.33	7.69	146.12	0.50	-8.97	-90.71	0.00	18.73	0.00
1	308.15	3,000	237.04	7.69	146.26	0.50	-8.97	-90.71	0.14	18.75	17.46
2	335.15	3,000	189.54	7.69	258.63	0.85	-27.43	-92.21	4.73	33.15	606.72
3	335.15	3,000	189.54	7.69	258.63	0.85	-27.43	-92.21	4.73	33.15	606.72
4	339.15	3,000	148.83	7.69	275.27	0.90	-30.96	-92.16	6.12	35.28	784.62
5	339.15	3,000	148.83	7.69	275.27	0.90	-30.96	-92.16	6.12	35.28	784.62
6	310.15	3,085	101.33	7.47	154.42	0.53	-10.01	-90.37	0.03	19.24	3.29
7	308.15	3,085	101.33	7.47	146.10	0.50	-8.97	-90.05	0.00	18.20	0.00
8	310.15	45	101.33	0.22	155.08	0.53	-9.97	-115.24	0.06	0.56	0.22
9	308.15	45	101.33	0.22	146.72	0.51	-8.93	-114.77	0.04	0.53	0.13

η_{pump} —pump efficiency (dimensionless), ρ —density of the fluid (kg/m^3), \dot{m} —mass flow rate of the fluid (kg/m^3).

There is no commonly agreed method for defining the solar exergy input because: (1) some assume that the exergy should be based on the radiation at the sun surface and thus at this temperature, of about 5,800 K, or just assuming that this electromagnetic radiation is pure exergy, and then some take into consideration the effects of the radiation cone solid angle between the sun and earth, and the incidence angle on the collector, and the solar radiation extinction by the atmosphere, all of which vary with time, or (2) others assume that the solar exergy input is just that of the solar heat at its input point to the system, for example the exergy of the solar-heated fluid at state 4 in Fig. 16 [50]. Banat et al. [48] used the commonly used expression based on the sun surface temperature:

$$\dot{E}_{sun} = A\dot{e}_{sun} = AI \left[1 + \frac{1}{3} \left(\frac{T_0}{T_{sun}} \right)^4 - \frac{4}{3} \left(\frac{T_0}{T_{sun}} \right) \right] \quad (134)$$

where \dot{e}_{sun} is exergy of the solar irradiation per unit area (W/m^2), T_0 —dead state temperature (K), T_{sun} —temperature of the sun surface (K), which is considered in [48] to be 6,000 K.

An alternate expression for calculating the solar irradiation exergy, based on the temperature of the solar-heated fluid is [50]:

$$\dot{E}_{sun} = A\dot{e}_{sun} = AI \left(1 - \frac{T_0}{T_4} \right) \quad (135)$$

where T_4 is fluid temperature at the solar collector outlet, state 4 (K).

The solar exergy associated with the solar thermal collector can be calculated by using either Eqs. (134) or (135), so as to demonstrate the difference in the results in using these two solar heat exergy definition methods, the exergy analysis is once done using Eq. (134) and repeated by using Eq. (135). Eq. (134) is used to calculate the exergy efficiency of the PV module in both approaches. We named the exergy of the solar irradiation calculated using Eq. (134) and its corresponding exergy efficiency of the solar collector \dot{E}_{sun}^{sun} and ψ_{sc}^{sun} when based on the sun temperature, respectively. The exergy of the solar irradiation calculated using Eq. (135) and its corresponding exergy efficiency of the solar collector are named \dot{E}_{sun}^{flu} and ψ_{sc}^{flu} , respectively, based on the solar-heated fluid temperature. Based on Table 1, the solar irradiation I , solar collector area A_{sc} , PV panel area A_{PV} and Eqs. (129)–(135), the

calculated results are summarized in Table 2, demonstrating an order-of magnitude differences between the exergy values when calculated by the 2 methods. Both methods are fundamentally correct and their choice depends on the user's objective, and it is important to recognize their differences when comparing such results.

The total energy input for this system is considered to be the total solar irradiation $I(A_{sc} + A_{PV}) = 6,654.2 \text{ W}$. The solar irradiation supplied to the solar collector $IA_{sc} = 5,820.0 \text{ W}$ is considered as the heat input for the system, and the electrical power generated by the PV module $\dot{W}_e = 145.5 \text{ W}$ is considered as the electrical power consumption for the system. The latent heat of the feed solution used in the calculation is the average of the latent heats of states 5 and 6 ($\Delta H_{fg} = 2,370.8 \text{ kJ}/\text{kg}$).

The energy performance criteria applied and calculated for this system are: the Specific heat consumption SHC (Eq. (96)); the Specific electrical energy consumption $SEEC$ (Eq. (98)); the Membrane thermal efficiency η (Eqs. (50), (87) and (100)); the GOR (Eq. (102)); and the Heat recovery factor H_r (Eqs. (50), (52) and (104)). The GOR and heat recovery factor are calculated neglecting supercooling and superheating in the heat exchanger, because they weren't reported in [48]. The results are summarized in Table 3.

The solar collector heats the brackish water (state 3 to 4) for the MD process, and the solar irradiation is also used to generate electrical power by a PV module to drive the pump bringing the brackish water from state 0 to 1, the useful product is the distilled water (state 9), and the main byproduct is the concentrated brackish water effluent (state 7). It is obvious for this solar-driven system that reduction of the energy input per unit produced water is useful for reducing system and product cost, but energy analysis alone does not provide sufficient guidance for system improvement because the system uses and outputs different types of energy, which have different qualities, characterized by exergy. Starting with the solar irradiation input to the thermal and PV collectors, it consists of electromagnetic waves and is thus pure exergy and is a function of the sun surface temperature (Eq. (134)) [50]. The electrical power generated by the PV module is also pure exergy (Eq. (57)). The heat produced in the solar collector has an exergy that is a function of the heated fluid temperature and pressure (Eqs. (58)–(61)). The distillate, saline feed, and concentrated brackish water discharge have exergies that are a function of their temperatures, pressures, and compositions (Eqs. (58)–(61)). Energy analysis does not account for the energy flows' quality, and therefore, for example, one Watt of electrical power is assigned the same value as

Table 2
Energy and exergy performance of the PV module and solar collector

PV module			Solar collector		
Symbol	Equation or its number	Value	Symbol	Equation or its number	Value
I (W/m ²)		970.0	I (W/m ²)		970.0
A_{PV} (W/m ²)		0.9	A_{sc} (W/m ²)		6.0
\dot{W}_e (W)		145.5	$\dot{H}_4 - \dot{H}_3$ (W)		2,132.8
\dot{w}_e (W/m ²)	\dot{W}_e / A_{PV}	169.8	$\dot{E}_4 - \dot{E}_3$ (W)		177.9
\dot{E}_{sun} (W)	(134)	777.1	\dot{E}_{sc}^{sun} (W)	(134)	5,421.6
			\dot{E}_{sc}^{flu} (W)	(135)	532.0
\dot{e}_{sun} (W/m ²)	\dot{E}_{sun} / A_{PV}	903.6	\dot{e}_{sc}^{sun} (W/m ²)	$\dot{E}_{sc}^{sun} / A_{sc}$	903.6
			\dot{e}_{sc}^{flu} (W/m ²)	$\dot{E}_{sc}^{flu} / A_{sc}$	150.6
η_{PV} (%)	(131)	17.5	η_{sc} (%)	(129)	36.6
ψ_{PV} (%)	(132)	18.8	ψ_{sc}^{sun} (%)	(130)	3.3
			ψ_{sc}^{flu} (%)	(130)	33.4

Table 3
Energy performance of the system

Performance criterion	Equation number	Value
SHC (kJ/kg)	(96)	1,587.3
SEEC (kJ/kg)	(98)	39.7
η (%)	(50), (87), and (100)	54.2
GOR (dimensionless)	(102)	1.5
H_r (%)	(50), (52), and (104)	89.8

one Watt of low temperature heat while the work potential of one Watt of electrical power has one Watt of exergy while the Watt of the heat energy has an exergy value much lower than one Watt as determined by Eq. (56).

Based on the data in Tables 1 and 2, an exergy analysis of this system was conducted, including the calculation of the irreversibilities of the system, and thereby examined the potential for its improvement. As discussed above, two expressions for calculating the solar irradiation exergy were used. The total exergy input for this system is considered to be the exergy of the solar irradiation to the solar collector and PV module.

The exergy performance criteria applied and calculated for this system were: Overall exergy efficiency ψ_t (Eq. (113)); Utilitarian exergy efficiency ψ_u (Eq. (114)); Specific exergy consumption SXC (Eq. (116)); Exergy consumption ratio XCR (based on the thermodynamically minimal separation exergy to the actual used, Eq. (118)). When calculating the overall exergy efficiency, the total exergy input is the sum of the solar exergy input to the PV module ($\dot{E}_{sun} = 777.1$ W) and

solar collector ($\dot{E}_{sc}^{sun} = 5,421.6$ W or $\dot{E}_{sc}^{flu} = 532.0$ W), and the total exergy output is the flow exergy of distillate ($\dot{E}_9 = 0.13$ W) and concentrated brackish water ($\dot{E}_7 = 0.00$ W). As discussed further below, the solar collector and PV module are the main exergy destruction subprocesses of the system, so this system has lower overall exergy efficiency than the system considered MD separation subprocess only reported in [48].

To compare our results with the exergy analysis done in [48], we make the same assumptions as they did, but replace the method used to calculate the flow exergy by the method proposed in [49], since some negative flow exergy values were given in [48], indicating that their method may have some errors. Their analysis did not consider the PV module and the flow system pressure changes, and unlike here, they assumed that the exergy input for the system equals to the flow exergy difference of state 3 and 4. Based on these assumptions and our calculation of the flow exergy, our result is that the exergy input is 183.19 W and $\psi_t = 0.072\%$, $\psi_u = 0.070\%$, $XCR = 0.072\%$. Ref. [48] reported that $\psi_t = 0.3\%$, different from our result since a different method was used to calculate the flow exergy.

When calculating the utilitarian exergy efficiency (ψ_u), the solar irradiation exergy input to the solar collector and PV module is considered as the valuable exergy input, and the flow exergy of the desired distilled water product is considered to be the valuable exergy output. When calculating the Exergy consumption ratio, SXC_{min} is calculated by Eq. (120) with thermodynamic property correlations reported in [34] and thus $SXC_{min} = 0.036$ kJ/kg.

The results are summarized in Table 4, showing that the results for the exergy performance are significantly different, depending on the expressions used to calculate the solar irradiation exergy to the solar collector. In both expressions used in this paper, a negligible portion of the input exergy is carried out by the desired product.

Next, energy and exergy analyses are conducted on the five subprocesses of the system: first considered is the solar collector subprocess (dashed rectangle denoted by A in Fig. 16) where the feed stream is heated by the solar irradiation, second is the MD separation subprocess (dashed rectangle denoted by B in Fig. 16), third is the PV module subprocess (dashed rectangle denoted by C in Fig. 16) where solar irradiation is used to generate electrical power, fourth is the pump subprocess (dashed rectangle denoted by D in Fig. 16) where electrical power is supplied to drive the pump, fifth is the discharge subprocess (dashed rectangle denoted by E in Fig. 16) where the distilled and concentrated brackish water streams leave the MD module and are cooled to ambient temperature.

The energy analysis results of these subprocesses are summarized in Table 5. Process energy efficiency is defined as the ratio of the energy output to the energy input. It should be noted this process energy efficiency for the solar collector is different from the commonly defined energy efficiency of the solar collector, η_{sc} . The process energy efficiency is calculated by:

$$\eta_{sub} = \frac{\dot{E}_{out,sub}}{\dot{E}_{in,sub}} \tag{136}$$

where η_{sub} —process energy efficiency of the subprocess (dimensionless), $\dot{E}_{out,sub}$ —energy output of the subprocess (W), $\dot{E}_{in,sub}$ —energy input of the subprocess (W).

The energy loss to the environment of the subprocess is defined as the energy difference between energy input and output of the subprocess and it is calculated by:

$$\dot{E}_{loss,sub} = \dot{E}_{in,sub} - \dot{E}_{out,sub} \tag{137}$$

where $\dot{E}_{loss,sub}$ is subprocess energy loss to the environment (W), $\dot{E}_{out,sub}$ —subprocess energy output (W), $\dot{E}_{in,sub}$ —subprocess energy input (W).

The relative energy loss to the environment is defined as energy loss to the environment of the subprocess to the total energy input and is calculated by:

$$lr_{sub} = \frac{\dot{E}_{loss,sub}}{\dot{E}_{input}} \tag{138}$$

where lr_{sub} is subprocess relative energy loss to the environment (dimensionless), $\dot{E}_{loss,sub}$ —subprocess energy loss to the environment (W), \dot{E}_{input} —total energy input (W).

The total energy input to the system are the solar irradiation ($I(A_{sc} + A_{PV}) = 6,654.2 \text{ W}$) plus the enthalpy of the feed solution input (\dot{H}_0), while the energy output of the system are the enthalpy of the distilled water and concentrated brackish water. It was found that about 73.8% of the energy input is carried out by the product and byproduct liquids. The flow enthalpy of the distillate (\dot{H}_9) amounts to 2.1% of the total energy input and the flow enthalpy of the concentrated brackish water (\dot{H}_7) amounts to 71.7% of the total energy input. According to the fluid properties in Table 1, it is noteworthy that in this example the combined enthalpy of the output distilled water (146.72 kJ/kg) and of the concentrated brackish water (146.10 kJ/kg) have nearly the same enthalpy as the input feed solution (146.12 kJ/kg), so the heat loss of the system to the environment equals to the input energy from the solar irradiation. In these energy losses to environment, the solar collector process consists of 55.4% of the total heat loss to the environment, which is the major energy loss process of this system. The distribution for the total energy input among the subprocesses is shown in Fig. 18.

Based on the fluid properties in Table 1 and performance of the PV module and solar collector in

Table 4
Exergy performance of the system

Performance criterion	Equation number	Solar exergy calculated based on	
		Sun temperature	Fluid temperature
ψ_t (%)	(113)	0.0021	0.010
ψ_u (%)	(114)	0.0021	0.0098
SXC (kJ/kg)	(116)	1,690.5	357.0
XCR (%)	(118)	0.0021	0.010

Table 5
Energy analysis of the subprocess

Process	Energy input, $\dot{E}_{in,sub}$		Energy output, $\dot{E}_{out,sub}$		Energy loss to environment, $\dot{E}_{loss,sub}$		Process energy efficiency, η_{sub}		Relative energy loss to environment, Ir_{sub}	
	Equation	Value (kW)	Equation	Value (kW)	Equation	Value (kW)	Equation	Value (%)	Equation	Value (%)
Solar collector	$IA_{sc} + \dot{H}_2$	39.0	\dot{H}_5	35.3	$IA_{sc} + \dot{H}_2 - \dot{H}_5$	3.7	$\dot{H}_5 / (IA_{sc} + \dot{H}_2)$	90.5	$(IA_{sc} + \dot{H}_2 - \dot{H}_5) / [(A_{sc} + A_{pv}) + \dot{H}_2]$	14.5
MD separation	$\dot{H}_1 + \dot{H}_5$	54.0	$\dot{H}_2 + \dot{H}_6 + \dot{H}_8$	52.9	$\dot{H}_1 + \dot{H}_5 - \dot{H}_2 - \dot{H}_6 - \dot{H}_8$	1.1	$(\dot{H}_2 + \dot{H}_6 + \dot{H}_8) / (\dot{H}_1 + \dot{H}_5)$	98.0	$(\dot{H}_1 + \dot{H}_5 - \dot{H}_2 - \dot{H}_6 - \dot{H}_8) / [(A_{sc} + A_{pv}) + \dot{H}_2]$	4.3
PV module Pump	IA_{pv}	0.8	\dot{W}_e	0.1	$IA_{pv} - \dot{W}_e$	0.7	\dot{W}_e / IA_{pv}	17.4	$(IA_{pv} - \dot{W}_e) / [(A_{sc} + A_{pv}) + \dot{H}_2]$	2.7
	$\dot{H}_0 + \dot{W}_e$	18.9	\dot{H}_1	18.7	$\dot{H}_0 + \dot{W}_e - \dot{H}_1$	0.1	$\dot{H}_1 / (\dot{H}_0 + \dot{W}_e)$	99.3	$(\dot{H}_0 + \dot{W}_e - \dot{H}_1) / [(A_{sc} + A_{pv}) + \dot{H}_2]$	0.5
Discharge	$\dot{H}_6 + \dot{H}_8$	19.8	$\dot{H}_7 + \dot{H}_9$	18.7	$\dot{H}_6 + \dot{H}_8 - \dot{H}_7 - \dot{H}_9$	1.1	$(\dot{H}_7 + \dot{H}_9) / (\dot{H}_6 + \dot{H}_8)$	94.6	$(\dot{H}_6 + \dot{H}_8 - \dot{H}_7 - \dot{H}_9) / [(A_{sc} + A_{pv}) + \dot{H}_2]$	4.2
Total	I $(A_{sc} + A_{pv}) + \dot{H}_2$	25.4	$\dot{H}_7 + \dot{H}_9$	18.7	I $(A_{sc} + A_{pv}) + \dot{H}_2 - \dot{H}_7 - \dot{H}_9$	6.7	$(\dot{H}_7 + \dot{H}_9) / [I (A_{sc} + A_{pv}) + \dot{H}_2]$	73.8	$[I (A_{sc} + A_{pv}) + \dot{H}_2 - \dot{H}_7 - \dot{H}_9] / [I (A_{sc} + A_{pv}) + \dot{H}_2]$	1.2

Table 2, the exergy analysis of these subprocesses, based separately on the two expressions for calculating the solar irradiation exergy are summarized in Tables 6 and 7. The exergy efficiency is defined here as the ratio of the exergy input to the exergy output of the subprocess and is calculated by:

$$\psi_{sub} = \frac{\dot{E}_{out,sub}}{\dot{E}_{in,sub}} \quad (139)$$

where ψ_{sub} is exergy efficiency of the subprocess (dimensionless), $\dot{E}_{out,sub}$ —exergy output of the subprocess (W), $\dot{E}_{in,sub}$ —exergy input of the subprocess (W).

The exergy destruction by a subprocess is defined as the exergy difference between exergy input and exergy output of the subprocess and is calculated by:

$$\dot{E}_{des,sub} = \dot{E}_{in,sub} - \dot{E}_{out,sub} \quad (140)$$

where $\dot{E}_{des,sub}$ is exergy destruction of the subprocess (W), $\dot{E}_{in,sub}$ —exergy input of the subprocess (W), $\dot{E}_{out,sub}$ —exergy output of the subprocess (W).

The relative exergy destruction ratio is calculated by Eq. (125).

It can be seen from Tables 6 and 7 that a negligible portion of the input exergy is carried out by the products, which is contrary to the result of the energy analysis and is one demonstration of the of their differences. When the solar exergy supplied to the solar collector is calculated based on the sun temperature, the exergy destruction in the solar collector process amounts to 84.6% of the total exergy destruction,

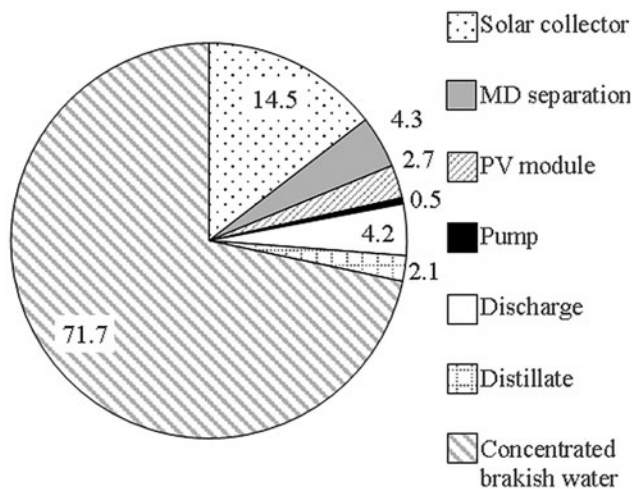


Fig. 18. System energy input distribution with % breakdown by the system subprocesses (percentage).

while when it is calculated based on the fluid temperature, the exergy destruction in the PV module process amounts to only 48.3% of the total exergy destruction, but is still the main exergy destruction in the system. The calculation thus demonstrates that the expressions used to calculate the solar exergy strongly influence the exergy analysis results. Figs. 19 and 20 show the exergy destruction shares when using these two expressions of the solar irradiation exergy.

Keeping in mind that the main purpose of this example is to show how exergy analyses are made and how they and their results differ from energy analyses, some key conclusions about the exergy and energy performance of this sample system can also be drawn:

- (1) 73.8% of the input energy is carried out by the distillate and concentrated brackish water, and 26.2% of the total energy is lost to the environment.
- (2) The exergy analysis shows, however, that a negligible amount of exergy is carried out by the product and byproducts, mainly because they are near the dead state temperature.
- (3) The solar collector energy conversion process is responsible for 55.4% of the total energy loss to the environment.
- (4) The exergy analysis results depend strongly on the choice of the expression for calculating the solar exergy input:
 - (a) If the solar exergy supplied to the solar collector is calculated based on the sun temperature, Eq. (134), the exergy destruction in the solar collector amounts to 84.6% of the total exergy destruction in the system. One of the conclusions from this result is that the use of solar radiation generated at the sun temperature for producing low temperature heat is thermodynamically very inefficient.
 - (b) If the solar exergy supplied to the solar collector is calculated based on the inlet fluid temperature, Eq. (135), the PV module process causes 48.3% of the total exergy destruction, which is also the largest component exergy destruction in the system. The second largest exergy destroyer in this approach is the solar collector, which accounts for 27.1% of the total exergy destruction.
- (5) The energy analysis, which points thus to the suggestion that increasing the energy efficiency of the solar collector would contribute most to the overall system energy efficiency.

Table 6
Exergy analysis of the subprocesses, with the solar irradiation exergy to the solar collector calculated based on the sun temperature (Eq. (134))

Process	Exergy input, $\dot{E}_{in,sub}$		Exergy output, $\dot{E}_{out,sub}$		Exergy destruction, $\dot{E}_{loss,sub}$		Exergy efficiency, η_{sub}		Relative exergy destruction ratio, XDR	
	Equation	Value (W)	Equation	Value (W)	Equation	Value (W)	Equation	Value (%)	Equation	Value (%)
Solar collector	$\dot{e}_{sc}^{sun} A_{sc} + \dot{E}_2$	6,028.2	\dot{E}_5	784.6	$\dot{e}_{sc}^{sun} A_{sc} + \dot{E}_2 - \dot{E}_5$	5,243.6	$\dot{E}_5 / (\dot{e}_{sc}^{sun} A_{sc} + \dot{E}_2)$	13.0	$(\dot{e}_{sc}^{sun} A_{sc} + \dot{E}_2 - \dot{E}_5) / (\dot{e}_{sc}^{sun} A_{sc} + \dot{e}_{sum} A_{pv} + \dot{E}_2)$	84.6
MD separation	$\dot{E}_1 + \dot{E}_5$	802.1	$\dot{E}_2 + \dot{E}_6 + \dot{E}_8$	610.2	$\dot{E}_1 + \dot{E}_5 - \dot{E}_2 - \dot{E}_6 - \dot{E}_8$	191.8	$(\dot{E}_2 + \dot{E}_6 + \dot{E}_8) / (\dot{E}_1 + \dot{E}_5)$	76.1	$(\dot{E}_1 + \dot{E}_5 - \dot{E}_2 - \dot{E}_6 - \dot{E}_8) / (\dot{e}_{sc}^{sun} A_{sc} + \dot{e}_{sum} A_{pv} + \dot{E}_2)$	3.1
PV module	$\dot{e}_{sum} A_{pv}$	777.1	\dot{W}_e	145.5	$\dot{e}_{sum} A_{pv} - \dot{W}_e$	631.6	$\dot{W}_e / \dot{e}_{sum} A_{pv}$	18.7	$(\dot{e}_{sum} A_{pv} - \dot{W}_e) / (\dot{e}_{sc}^{sun} A_{sc} + \dot{e}_{sum} A_{pv} + \dot{E}_2)$	10.2
Pump	$\dot{E}_0 + \dot{W}_e$	145.5	\dot{E}_1	17.5	$\dot{E}_0 + \dot{W}_e - \dot{E}_1$	128.0	$\dot{E}_1 / (\dot{E}_0 + \dot{W}_e)$	12.0	$(\dot{E}_0 + \dot{W}_e - \dot{E}_1) / (\dot{e}_{sc}^{sun} A_{sc} + \dot{e}_{sum} A_{pv} + \dot{E}_2)$	2.1
Discharge	$\dot{E}_6 + \dot{E}_8$	3.5	$\dot{E}_7 + \dot{E}_9$	0.1	$\dot{E}_6 + \dot{E}_8 - \dot{E}_7 - \dot{E}_9$	3.4	$(\dot{E}_7 + \dot{E}_9) / (\dot{E}_6 + \dot{E}_8)$	3.7	$(\dot{E}_6 + \dot{E}_8 - \dot{E}_7 - \dot{E}_9) / (\dot{e}_{sc}^{sun} A_{sc} + \dot{e}_{sum} A_{pv} + \dot{E}_2)$	0.0
Total	$\dot{e}_{sc}^{sun} A_{sc} + \dot{e}_{sum} A_{pv} + \dot{E}_2$	6,198.6	$\dot{E}_7 + \dot{E}_9$	0.1	$\dot{e}_{sc}^{sun} A_{sc} + \dot{e}_{sum} A_{pv} + \dot{E}_2 - \dot{E}_7 - \dot{E}_9$	6,198.4	$(\dot{E}_7 + \dot{E}_9) / (\dot{e}_{sc}^{sun} A_{sc} + \dot{e}_{sum} A_{pv} + \dot{E}_2)$	0.0	$(\dot{e}_{sc}^{sun} A_{sc} + \dot{e}_{sum} A_{pv} + \dot{E}_2 - \dot{E}_7 - \dot{E}_9) / (\dot{e}_{sc}^{sun} A_{sc} + \dot{e}_{sum} A_{pv} + \dot{E}_2)$	100.0

Table 7
Exergy analysis of the subprocesses, with the solar irradiation exergy to the solar collector calculated based on the fluid temperature (Eq. (135))

Process	Exergy input, $\dot{E}_{in,sub}$		Exergy output, $\dot{E}_{out,sub}$		Exergy destruction, $\dot{E}_{loss,sub}$		Exergy efficiency, ψ_{sub}		Relative exergy destruction ratio, XDR	
	Equation	Value (W)	Equation	Value (W)	Equation	Value (W)	Equation	Value (%)	Equation	Value (%)
Solar collector	$\dot{e}_{sc}^{flu} A_{sc} + \dot{E}_2$	1,138.7	\dot{E}_5	784.6	$\dot{e}_{sc}^{flu} A_{sc} + \dot{E}_2 - \dot{E}_5$	354.1	$\dot{E}_5 / (\dot{e}_{sc}^{flu} A_{sc} + \dot{E}_2)$	68.9	$(\dot{e}_{sc}^{flu} A_{sc} + \dot{E}_2 - \dot{E}_5) / (\dot{e}_{sc}^{flu} A_{sc} + \dot{e}_{sum} A_{pv} + \dot{E}_2)$	27.0
MD separation	$\dot{E}_1 + \dot{E}_5$	802.1	$\dot{E}_2 + \dot{E}_6 + \dot{E}_8$	610.2	$\dot{E}_1 + \dot{E}_5 - \dot{E}_2 - \dot{E}_6 - \dot{E}_8$	191.8	$(\dot{E}_2 + \dot{E}_6 + \dot{E}_8) / (\dot{E}_1 + \dot{E}_5)$	76.1	$(\dot{E}_1 + \dot{E}_5 - \dot{E}_2 - \dot{E}_6 - \dot{E}_8) / (\dot{e}_{sc}^{flu} A_{sc} + \dot{e}_{sum} A_{pv} + \dot{E}_2)$	14.7
PV module	$\dot{e}_{sum} A_{pv}$	777.1	W_e	145.5	$\dot{e}_{sum} A_{pv} - W_e$	631.6	$W_e / \dot{e}_{sum} A_{pv}$	18.7	$(\dot{e}_{sum} A_{pv} - W_e) / (\dot{e}_{sc}^{flu} A_{sc} + \dot{e}_{sum} A_{pv} + \dot{E}_2)$	48.2
Pump	$\dot{E}_0 + W_e$	145.5	\dot{E}_1	17.5	$\dot{E}_0 + W_e - \dot{E}_1$	128.0	$\dot{E}_1 / (\dot{E}_0 + W_e)$	12.0	$(\dot{E}_0 + W_e - \dot{E}_1) / (\dot{e}_{sc}^{flu} A_{sc} + \dot{e}_{sum} A_{pv} + \dot{E}_2)$	9.8
Discharge	$\dot{E}_6 + \dot{E}_8$	3.5	$\dot{E}_7 + \dot{E}_9$	0.1	$\dot{E}_6 + \dot{E}_8 - \dot{E}_7 - \dot{E}_9$	3.4	$(\dot{E}_7 + \dot{E}_9) / (\dot{E}_6 + \dot{E}_8)$	3.7	$(\dot{E}_6 + \dot{E}_8 - \dot{E}_7 - \dot{E}_9) / (\dot{e}_{sc}^{flu} A_{sc} + \dot{e}_{sum} A_{pv} + \dot{E}_2)$	0.3
Total	$\dot{e}_{sc}^{flu} A_{sc} + \dot{e}_{sum} A_{pv} + \dot{E}_2$	1,309.1	$\dot{E}_7 + \dot{E}_9$	0.1	$\dot{e}_{sc}^{flu} A_{sc} + \dot{e}_{sum} A_{pv} + \dot{E}_2 - \dot{E}_7 - \dot{E}_9$	1,308.9	$(\dot{E}_7 + \dot{E}_9) / (\dot{e}_{sc}^{flu} A_{sc} + \dot{e}_{sum} A_{pv} + \dot{E}_2)$	0.0	$[\dot{e}_{sc}^{flu} A_{sc} + \dot{e}_{sum} A_{pv} + \dot{E}_2 - \dot{E}_7 - \dot{E}_9] / (\dot{e}_{sc}^{flu} A_{sc} + \dot{e}_{sum} A_{pv} + \dot{E}_2)$	100.0

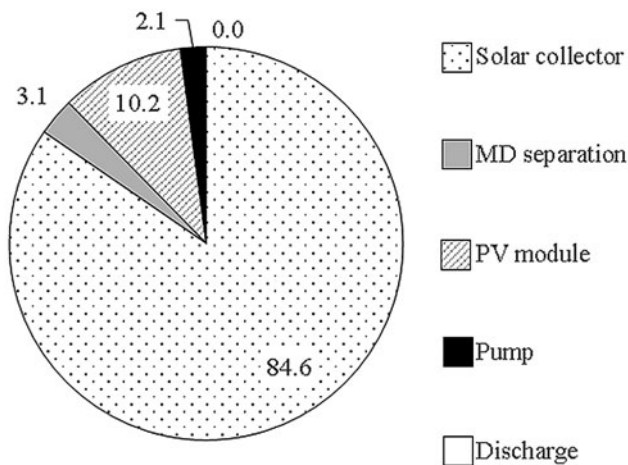


Fig. 19. System exergy destruction including % breakdown by its subprocesses (percentage) with the solar irradiation exergy of the solar collector is calculated based on sun temperature Eq. (134).

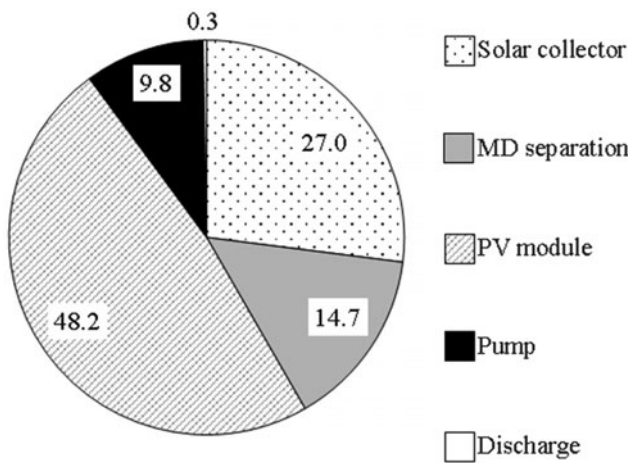


Fig. 20. System exergy destruction including % breakdown by its subprocesses (percentage) with the solar irradiation exergy of the solar collector calculated based on the fluid temperature Eq. (135).

- (6) The exergy analysis shows that the solar collector is also the major exergy destruction subprocess. Increasing the exergy efficiency of the solar collector would require increasing of the flow exergy of the heated fluid according to Eq. (130), where $\dot{E}_4 = \dot{m}_4 e_4$. Thus, for example, a solar collector delivering a fixed amount of heat: $IA_{sc} = \dot{m}_4 C_p (T_4 - T_3)$ can have different exergy efficiencies ψ_{sc} that depend ((Eq. (60)) on the collector outflow temperature T_4 , which, in turn would depend on the collector flow rate \dot{m}_4 .

Many constructive guidelines for improving system efficiency can thus be drawn from the exergy analysis, which are not revealed by energy analysis alone or at all. We note that this example in Section 3.6.7 is primarily intended to demonstrate the exergy analysis method, and the conclusions from the analyses results are left to the user.

3.7. Heat and mass transport analysis

The performance criteria used to characterize the transport process in MD are discussed in this section. These criteria are generally about the membrane module, where the coupled mass and heat transfer for the separation takes place. For an MD system shown in Fig. 8, the control volume of the membrane module considered in the definitions of the transport analysis performance criteria is outlined by the dashed line of B in Fig. 15.

3.7.1. The convective heat transfer coefficient for fluid flow (h)

Here the well-known convective heat transfer coefficient, defined as the ratio of the total heat flux to the temperature difference between two points or surfaces in a fluid or between a point or surface in the fluid and another point or surface on a solid-fluid interface. In MD that interface is the membrane or the solid planes (such cooling plane) and the fluid could be the feed stream, the permeate stream, or the coolant stream. It is defined as follow:

$$h = \frac{q_t''}{T_b - T_{inter}} \quad (141)$$

where h is convective heat transfer coefficient between defined points and/or surfaces ($W/(m^2 K)$), q_t'' —total heat flux there (W/m^2), T_b —temperature at a chosen location in the bulk flow (K), T_{inter} —temperature at the chosen heat transfer boundary (K).

On the membrane module level (B in Fig. 15), as discussed in Section 2.2, heat transfer in the fluid streams are essential components of the overall heat transfer process in MD and the thermal boundary layer of the fluid stream imposes an important portion of the total heat transfer resistance [4], in large part characterized by h . Increasing h reduces the overall heat transfer resistance in the membrane module, which can be achieved through methods such as increasing the feed and the distillate stream flow velocities or the use of flow inserts (“spacers”) [11].

On the MD system level (Fig. 14), h also plays a key role in all other heat transfer related components in the system, such as the heat input and the recovery heat exchangers.

3.7.2. Nusselt number (Nu)

The well-known Nusselt number is defined as the ratio of the convective to conductive heat transfer fluxes across the chosen boundaries of the fluid stream.

$$Nu = \frac{h \cdot d}{k_f} \tag{142}$$

where Nu is Nusselt number (dimensionless), h —convective heat transfer coefficient ($W/(m^2 K)$), d —stream hydraulic diameter (m), k_f —thermal conductivity of fluid ($W/(m K)$).

Correlations exist to relate Nu to easily measurable dimensionless number such as the flow Reynolds number (Re) and the fluid Prandtl number (Pr), allowing the determination of h [11,51,52].

3.7.3. Temperature polarization coefficient (TPC)

The temperature polarization coefficient is defined as the ratio of the temperature difference across the membrane surfaces to the temperature difference between the feed and the permeate bulk streams:

$$TPC = \frac{T_{f,m} - T_{p,m}}{T_f - T_p} \tag{143}$$

where TPC is temperature polarization coefficient (dimensionless), $T_{f,m}$ —temperature at the membrane feed-side surface (K), $T_{p,m}$ —temperature at the membrane permeate-side surface (K), T_f —temperature of the feed bulk (K), T_p —temperature of the permeate bulk (K).

The related temperature used to calculate the TPC for DCMD and AGMD are shown in Figs. 3 and 5.

TPC is the ratio of the actual temperature driving force across the membrane to the present theoretical maximal temperature driving force across it. To keep the coherent physical meaning and standardizing the TPC value among all MD configurations, Alsaadi et al. [53] proposed that the most appropriate definition for TPC in VMD is:

$$TPC = \frac{T_{f,m} - T_v^*}{T_f - T_v^*} \tag{144}$$

where T_v^* is saturation temperature of the vacuum side vapor pressure (K).

Noted that T_v is the actual temperature at the vacuum side membrane surface, and T_v^* is not the actual temperature as shown in Fig. 21.

In SGMD, the vapor is condensed by an external condenser and the vapor pressure of sweeping gas stream can be below its saturated pressure, so similar as TPC is defined in VMD, the TPC in SGMD is defined as:

$$TPC = \frac{T_{f,m} - T_{p,m}^*}{T_f - T_p^*} \tag{145}$$

where $T_{p,m}^*$ is saturation temperature of the vapor pressure at the membrane surface of the sweeping gas side (K), T_p^* —saturation temperature of the vapor pressure at the bulk of the sweeping gas side (K).

Fig. 22 illustrates the definition of TPC in SGMD. Noted that $T_{p,m}$ is the actual temperature at the sweeping gas side membrane surface.

TPC can be a local value at any position typically used in transport process analysis and modeling or an average value of the whole MD membrane module.

The driving force for separation in MD is the cross-membrane vapor pressure difference generally generated by the temperature difference, so $(T_f - T_p)$ is the theoretical maximal driving force. The heat transfer rate from the feed to the coolant between these temperatures is limited by the resistances due to convection and conduction phenomena in the intervening media. These resistances cause corresponding drops in temperatures, as shown in Figs. 4 and 6, and as quantified by Eqs. (7) and (8). TPC is thus the ratio of the actual temperature driving force for the process to the maximal present driving force. According to the heat transfer resistance analog, TPC can also be evaluated by the heat transfer resistance of the membrane together with the other heat transfer resistance in the transport process. So as discussed in Section 2.2, TPC in DCMD can be calculated by:

$$TPC = \frac{T_{f,m} - T_{p,m}}{T_f - T_p} = \frac{1/H_m}{1/h_f + 1/H_m + 1/h_p} \tag{146}$$

In AGMD, additional heat transfer resistances are present due to the air gap (R_g), the condensate liquid film (R_p), and the cooling plate (R_c) are presented (Fig. 6) so:

$$TPC = \frac{T_{f,m} - T_{p,m}}{T_f - T_p} = \frac{1/H_m}{1/h_f + 1/H_m + R_g + R_p + R_c + 1/h_p} \tag{147}$$

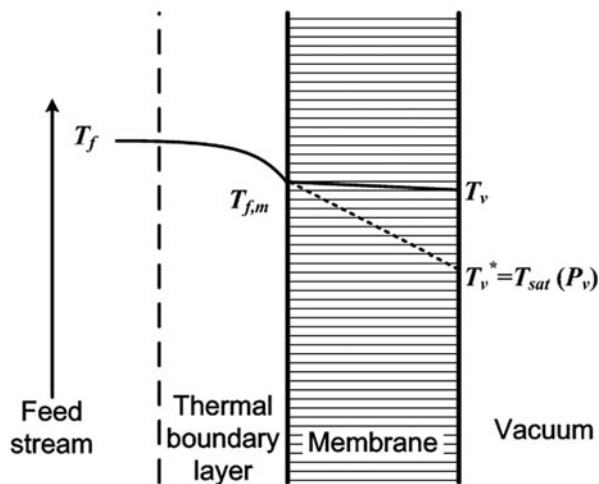


Fig. 21. Polarization definition-related temperature profiles in VMD.

In VMD and SGMD, the vapor is condensed by the external condenser as stated before, so this heat transfer resistance analysis cannot be simply applied to these processes.

TPC is often used as a criterion that evaluates the effects of heat transfer resistance of the thermal boundary layers relative to total heat transfer resistance. *TPC* rising to approach 1 indicates an increasing convective heat transfer coefficient and small heat transfer resistance of the intervening media, and the opposite is for *TPC* approaching zero.

3.7.4. Concentration polarization coefficient (CPC)

The concentration polarization coefficient is defined as the ratio of the molar concentration difference between the two membrane surfaces, to the

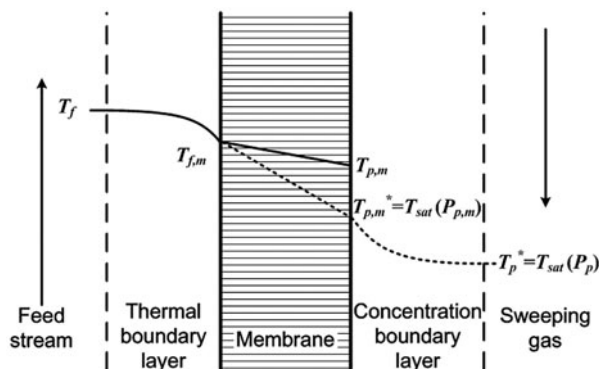


Fig. 22. Polarization definition-related temperature profiles in SGMD.

molar concentration difference between their molar concentrations in the feed and the permeate bulk streams.

$$CPC = \frac{c_{f,m} - c_{p,m}}{c_f - c_p} \quad (148)$$

where *CPC* is molar concentration polarization coefficient (dimensionless), $c_{f,m}$ —molar concentration at the membrane feed-side surface (mol/m^3), $c_{p,m}$ —molar concentration at the membrane permeate-side surface (mol/m^3), c_f —molar concentration of the feed bulk (mol/m^3), c_p —molar concentration of the permeate bulk (mol/m^3).

Typically, for non-volatile solutes, $c_{f,m}$ and c_f are equal to 0 for ideal MD process, since they are pure distillate, so then the equation is reduced to:

$$CPC = \frac{c_{f,m}}{c_f} \quad (149)$$

Typically in MD, volatile solvent flows across the membrane as vapor and non-volatile solutes are rejected at the membrane feed-side surface. As the solvent evaporates at the membrane feed-side surface, the concentration of the solutes increases and becomes higher at the membrane feed-side surface than in the bulk stream. This phenomenon is called concentration polarization. Similarly, the concentration polarization could also develop at the permeate side when the solute is volatile as Fig. 23 shows.

Similar to *TPC*, *CPC* quantifies the concentration polarization phenomenon exists in MD membrane module, and *CPC* was calculated from a film model [11].

$$CPC = \frac{c_{f,m}}{c_f} = \exp\left(\frac{J}{\rho_d k_{so}}\right) \quad (150)$$

where J is mass flux ($\text{kg}/(\text{m}^2 \text{s})$), ρ_d —density of the distillate (kg/m^3), k_{so} —mass transfer coefficient of the solutes (m/s).

Due to the concentration polarization, the mole fraction of solutes is higher at the feed/membrane interface, which decrease the vapor pressure compared to bulk condition and consequently reduces the distillation driving force. Moreover, higher concentration at the membrane may promote the scaling formed on the membrane and cause loss of hydrophobicity.

Analogy of the heat and mass transport processes indicates that methods that enhance heat transfer in fluid flow, such as increase of the flow velocity, and

use of flow inserts, will also enhance the species transfer and thus reduce the concentration polarization [54,55].

CPC is a criterion used to evaluate the transport process in MD, which is related to the product production rate, the energy efficiency, and the product quality.

3.7.5. Vapor pressure polarization coefficient (PPC)

The vapor pressure polarization coefficient is defined as the ratio of the vapor pressure difference between the two membrane surfaces to the vapor pressure difference in the feed and the permeate bulk streams.

$$PPC = \frac{p_{f,m} - p_{p,m}}{p_f - p_p} \quad (151)$$

where *PPC* is vapor pressure polarization coefficient (dimensionless), $p_{f,m}$ —vapor pressure at the membrane feed-side surface (Pa), $p_{p,m}$ —vapor pressure at the membrane permeate-side surface (Pa), p_f —vapor pressure of the feed bulk (K), p_p —vapor pressure of the permeate bulk (K).

MD is a thermally driven process utilizes vapor pressure difference at different temperature, and the mass flux is driven by vapor pressure difference as Eq. (9) indicates. So *PPC* is the ratio of the actual vapor pressure driving force for the process to the present maximal vapor pressure driving force, considering both the temperature polarization and the concentration polarization. *PPC* is applicable for all the four membrane module configurations, and was used, for example, to investigate MD in [56].

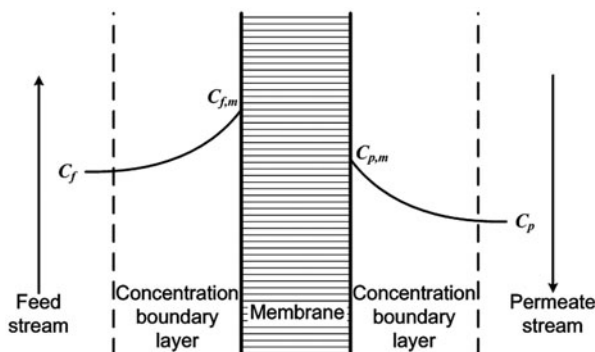


Fig. 23. Concentration polarization-definition related concentration profile.

3.8. Long-time performance criteria

MD productivity and energy/exergy efficiency deteriorate with operating time, mainly due to membrane properties changes and fouling. Long-time performance of MD thus must be evaluated, especially when for commercial applicability. Performance criteria used to evaluate the long-time performance of MD are discussed in this section.

3.8.1. Mass flux change rate (MCR)

The *mass flux change rate* is defined as the rate of the mass flux change as a percentage of the initial mass flux:

$$MCR = \frac{J_{initial} - J_{final}}{J_{initial}} \times \frac{1}{t} \quad (152)$$

where *MCR* is mass flux change rate (s^{-1}), $J_{initial}$ —initial mass flux ($kg/(m^2 s)$), J_{final} —final mass flux ($kg/(m^2 s)$), t —time period (s).

Many studies reported mass flux changes with time [57–65] due to deterioration of membrane materials, fouling, or the instability of the energy source (such as solar heat). Stability of membrane materials and fouling are an important aspect of MD system distillation rate, product quality, and energy efficiency. This criterion provides a comparative metric to evaluate MD performance in long-time operation with respect to the distillate production rate and factors that will influence MD distillate production rate in long-time operation.

3.8.2. Energy efficiency change rate (ECR)

Similar to changes in distillation rate, the energy efficiency may change with time too, so a criterion named “energy efficiency change rate” that evaluates the long-time operation effect on energy efficiency of the MD process is proposed here and is defined as the rate of *SHC* change as a percentage of the initial *SHC*.

$$ECR = \frac{SHC_{initial} - SHC_{final}}{SHC_{initial}} \times \frac{1}{t} \quad (153)$$

where *ECR* is energy efficiency change rate (s^{-1}), $SHC_{initial}$ —initial specific heat consumption (J/kg), SHC_{final} —final specific heat consumption (J/kg), t —time period (s).

MD energy efficiency changes with time have been reported in [48,57]. This criterion provides a comparative metric to evaluate MD performance in long-time

Table 8
Summary of the MD performance criteria with their utility

Index	Name	Symbol	Units	Equation number	Utility; evaluates the:
1	Basic membrane properties	–	–	–	Membrane's basic properties affect its performance in MD
2	Liquid entry pressure	LEP	Pa	(77)	Membrane's ability to prevent pore wetting
3	Membrane permeability	C	kg/(m ² s Pa)	(79)	Membrane's ability to produce mass flux
4	Mass transport pre-factor	PF	m ⁻¹ or dimensionless or m	(80)	Membrane's ability to produce mass flux just from membrane properties
5	Conduction heat transfer coefficient of the membrane	h_m	W/(m ² K)	(84)	Membrane's ability for the conduction heat loss
6	Product mass flow rate	\dot{m}_{pro}	kg/s	(85)	Product production rate
7	Mass flux	J	kg/(m ² s)	(87)	Transmembrane mass transfer rate per unit membrane area
8	Relative concentration change rate	CR	s ⁻¹	(89)	Concentration rate of the solution
9	Volumetric molar concentration	c	mol/m ³	(91)	Species concentration of the solution
10	Rejection factor	R	Dimensionless	(93)	Ratio of the solutes concentration difference between the feed solution and the distillate
11	Concentration factor	CF	Dimensionless	(94)	Concentration of the feed solution being concentrated or of the volatile solutes being removed
12	Separation factor	α	Dimensionless	(95)	Ability to separate the desired component
13	Specific heat consumption	SHC	J/kg or J/m ³	(96), (97)	Heat consumption to produce a unit mass or volume of the distillate
14	Specific electrical energy consumption	$SEEC$	J/kg or J/m ³	(98), (99)	Electrical energy consumption to produce a unit mass or volume of the distillate
15	Membrane thermal efficiency	η	Dimensionless	(100)	Heat utilization efficiency for distillation of the heat transport across the membrane
16	Gain output ratio	GOR	Dimensionless	(102)	Ratio of the transmembrane latent heat transfer rate to the heat input rate
17	Heat recovery factor	H_r	Dimensionless	(104)	Internal heat recovery extent in the MD system
18	Performance ratio	PR	Dimensionless	(105)	Ratio of the mass flow rate of the distillate to the mass flow rate of the input steam
19	Flow pressure drop	ΔP	Pa	(106)	pressure drop of the flow influencing the pump work and system operating conditions
20	Fuel energy saving ratio	$FESR$	Dimensionless	(107)	Ratio of the energy saved for dual-purpose desalination plant compare with separate power-only and water-only systems
21	Specific equivalent electrical energy consumption	$EEEC$	J/kg	(111), (112)	Electrical energy reduction of the dual-purpose desalination plant per unit mass or volume of the water produced
22	Overall exergy efficiency	ψ_t	Dimensionless	(113)	Overall thermodynamic irreversibility of the process
23	Utilitarian exergy efficiency	ψ_u	Dimensionless	(114)	Process exergy input and output based on user's need
24	Specific exergy consumption	SXC	J/kg	(116), (117)	Exergy consumption to produce a unit mass or volume of the product
25	Exergy consumption ratio	XCR	Dimensionless	(118)	Ratio of the minimum specific exergy consumption to the specific exergy consumption

(Continued)

Table 8 (Continued)

Index	Name	Symbol	Units	Equation number	Utility; evaluates the:
26	Exergy saving ratio	XSR	Dimensionless	(121)	Ratio of the exergy saved for dual-purpose desalination plant compare with separate power-only and water-only systems
27	Relative exergy destruction ratio	XDR	Dimensionless	(125)	Extent of the exergy destruction within the subsystem
28	Temperature driven heat flux kinetic coefficient	L_{11}'	W/(m K)	(46)	Contribution of unit temperature gradient to the heat flux
29	Concentration driven heat flux kinetic coefficient	L_{12}'	(W m ²)/mol	(46)	Contribution of unit concentration gradient to the heat flux
30	Temperature driven mass flux kinetic coefficient	L'_{21}	(kg K)/(m s)	(47)	Contribution of unit temperature gradient to the mass flux
31	Concentration driven mass flux kinetic coefficient	L'_{22}	(kg m ²)/(mol s)	(47)	Contribution of unit concentration gradient to the mass flux
32	Convective heat transfer coefficient for fluid flow	h	W/(m ² K)	(141)	Convective heat transfer ability of the fluid streams in MD
33	Nusselt number	Nu	Dimensionless	(142)	Ratio of the convective to conductive heat transfer ability of the fluid streams in MD
34	Temperature polarization Coefficient	TPC	Dimensionless	(143), (144), (145)	Driving temperature difference reduction across membrane due to heat transfer resistances in the module
35	Concentration polarization coefficient	CPC	Dimensionless	(148)	Concentration difference increase across membrane due to species transfer resistances in the module
36	Vapor pressure polarization coefficient	PPC	Dimensionless	(151)	Driving vapor pressure difference reduction across membrane due to heat and species transfer resistances in the module
37	Mass flux change rate	MCR	s ⁻¹	(152)	Distillation production rate change in the long-time operation
38	Energy efficiency change rate	ECR	s ⁻¹	(153)	Heat utilization efficiency change in the long-time operation
39	Product quality change rate	PCR	s ⁻¹	(154)	Product quality change in the long-time operation
40	Fouling rate	FR	s ⁻¹	(155), (156)	Fouling in the long-time operation and its impact on membrane properties

operation with respect to the heat utilization efficiency and factors that will influence MD energy performance in long-time operation.

3.8.3. Product quality change rate (PCR)

The product quality may also change with time, so a criterion named “product quality change rate” that evaluates the long-time operation effect on the quality of the product of MD process is proposed here and is defined as the rate of the solutes molar concentration

change of the product as a percentage of the initial solutes molar concentration of the product.

$$PCR = \frac{c_{initial} - c_{final}}{c_{initial}} \times \frac{1}{t} \quad (154)$$

where PCR is product quality change rate (s⁻¹), $c_{initial}$ —initial molar concentration of the solutes in product (mol/m³), c_{final} —final molar concentration of the solutes in product (mol/m³), t —time period (s).

Table 9

Summary of the performance criteria in MD classified by category of use in the MD system and by distinction between scientific and commercial types of application

Index	Name	Symbol	Categories		Application		
			Membrane	Module	Long System operation	Scientific Commercial	
1	Basic membrane properties	–	√			√	√
2	Liquid entry pressure	LEP	√			√	√
3	Membrane permeability	C	√			√	√
4	Mass transport pre-factor	PF	√			√	
5	Conduction heat transfer coefficient of the membrane	h_m	√			√	√
6	Product mass flow rate	\dot{m}_{pro}		√	√		√
7	Mass flux	J	√	√	√	√	√
8	Relative concentration change rate	CR		√	√	√	√
9	Volumetric molar concentration	c	√	√	√	√	√
10	Rejection factor	R	√	√	√	√	√
11	Concentration factor	CF		√	√	√	√
12	Separation factor	α		√	√	√	√
13	Specific heat consumption	SHC			√	√	√
14	Specific electrical energy consumption	SEEC			√	√	√
15	Membrane thermal efficiency	η	√	√		√	
16	Gain output ratio	GOR			√	√	√
17	Heat recovery factor	H_r			√	√	
18	Performance ratio	PR			√		√
19	Flow pressure drop	ΔP		√	√	√	√
20	Fuel energy saving ratio	FESR			√		√
21	Specific equivalent electrical energy consumption	EEEC			√		√
22	Overall exergy efficiency	ψ_t		√	√	√	√
23	Utilitarian exergy efficiency	ψ_u		√	√	√	√
24	Specific exergy consumption	SXC			√	√	√
25	Exergy consumption ratio	XCR			√	√	√
26	Exergy saving ratio	XSR			√		√
27	Relative exergy destruction ratio	XDR			√	√	√
28	Temperature driven heat flux kinetic coefficient	L'_{11}		√		√	
29	Concentration driven heat flux kinetic coefficient	L'_{12}		√		√	
30	Temperature driven mass flux kinetic coefficient	L'_{21}		√		√	
31	Concentration driven mass flux kinetic coefficient	L'_{22}		√		√	
32	Convective heat transfer coefficient for fluid flow	h		√		√	
33	Nusselt number	Nu		√		√	
34	Temperature polarization coefficient	TPC		√		√	
35	Concentration polarization coefficient	CPC		√		√	
36	Vapor pressure polarization coefficient	PPC		√		√	
37	Mass flux change rate	MCR			√	√	√
38	Energy efficiency change rate	ECR			√	√	√
39	Product quality change rate	PCR			√	√	√
40	Fouling rate	FR			√	√	√

The product quality change with time has been reported in MD [57,60,62,66]. This criterion provides a comparative metric to evaluate MD performance in long-time operation with respect to product quality and factors that will influence MD performance in long-time operation in that respect.

3.8.4. Fouling rate (FR)

Fouling in MD can be evaluated indirectly by the change rate of the operation performance (criteria *MCR*, *ECR*, *PCR*). It can also be evaluated and characterized more directly and specifically by the fouling itself and its impact on the membrane.

- (1) The fouling rate can be evaluated by the change rate of the surface concentration of the foulants. So the foulants change rate can be defined as the rate of the foulants surface concentration change as a percentage of the initial foulants surface concentration.

$$FR = \frac{c_{initial} - c_{final}}{c_{initial}} \times \frac{1}{t} \quad (155)$$

where *FR* is foulants change rate (s^{-1}), $c_{initial}$ —initial foulants surface concentration (mol/m^2), c_{final} —final foulants surface concentration (mol/m^2), t —time period (s).

It should be noticed that if the foulants are microorganisms, the foulants surface concentration is replaced in Eq. (155) by the number of the microorganisms per unit area:

$$FR = \frac{n_{initial} - n_{final}}{n_{initial}} \times \frac{1}{t} \quad (156)$$

where $n_{initial}$ is initial number of the microorganisms per unit area (m^{-2}), n_{final} —final number of the microorganisms per unit area (m^{-2}), t —time period (s).

- (2) The fouling rate can also be evaluated by the change rate of the membrane properties such as membrane thickness, porosity, contact angle, and tensile strength. Taking membrane thickness as an example, its change rate can be defined as the rate of the membrane thickness change as a percentage of the initial membrane thickness.

$$TCR = \frac{\delta_{initial} - \delta_{final}}{\delta_{initial}} \times \frac{1}{t} \quad (157)$$

where *TCR* is membrane thickness change rate (s^{-1}), $\delta_{initial}$ —initial membrane thickness (m), δ_{final} —final membrane thickness (m), t —time period (s).

Direct visual comparison also serves as a method to evaluate the fouling. More information about physical, chemical, and biological characterization techniques on fouling can be found in [67–69].

4. Conclusions

Table 8 summarizes the performance criteria reviewed in this paper with their units, definition equation numbers, and utilities. Table 9 summarizes these performance criteria, by category and application (scientific or commercial).

This report summarizes the technical/scientific performance criteria used in MD, on the component, module, and systems levels. It thus offers clarity and uniformity in their use.

While most of the surveyed performance criteria are in common use, some, especially those related to exergy analysis and criteria about long-time operation, are basically new.

Most of the performance criteria are based on universal scientific principles and widely used, but some have evolved with the technology for simplicity and convenience and may lack correct scientific principles and lack unique definitions. While it is not our objective to restrict their use, we pointed to their limitations. Furthermore, unnecessary duplicative multiplicity of performance criteria obfuscates the field, prevents scientific uniformity, and creates misunderstandings and misrepresentations. It is highly recommended to choose and use only the necessary minimum of performance criteria, based on uniform scientific criteria.

A full characterization of the membrane itself should include all the basic membrane properties listed. In MD, it is at least needed to include the *LEP*, the membrane permeability (*C*), and the conduction heat transfer coefficient of the membrane (h_m).

A comprehensive evaluation of the membrane module (and for research focused on the membrane when the evaluation is done with it installed in a module) and of the MD system should at least include evaluation of the production rate (Section 3.3), the product quality (Section 3.4) and the energy efficiency (Sections 3.5 and 3.6).

Other criteria were introduced to evaluate the transport process and the long-time operation, of special interest for commercial and industrial use.

Nomenclatures

A	— membrane area (m^2)	$H_{d,sat}$	— specific enthalpy of the saturated distillate (J/kg)
a	— activity of the solvent (dimensionless)	$H_{d,o}$	— specific enthalpy of the supercooled distillate (J/kg)
B	— geometric factor (dimensionless)	$H_{s,i}$	— specific enthalpy of the superheated steam (J/kg)
C	— membrane permeability ($\text{kg}/(\text{m}^2 \text{ s Pa})$)	$H_{s,sat}$	— specific enthalpy of the saturated steam (J/kg)
c	— volumetric molar concentration (mol/m^3) or foulants surface concentration (mol/m^2)	$H_{s,o}$	— specific enthalpy of the supercooled steam (J/kg)
CF	— concentration factor (dimensionless)	h_m	— conduction heat transfer coefficient of the membrane ($\text{W}/(\text{m}^2 \text{ K})$)
C_p	— specific heat capacity at constant pressure ($\text{J}/(\text{K kg})$)	H_m	— total heat transfer coefficient of the membrane, defined in Eq. (4) ($\text{W}/(\text{m}^2 \text{ K})$)
CPC	— concentration polarization coefficient (dimensionless)	H_r	— heat recovery factor (dimensionless)
CR	— relative concentration change rate (s^{-1})	$\dot{H}_{in,f}$	— enthalpy of the feed inflow (W)
C_v	— specific heat capacity at constant volume ($\text{J}/(\text{K kg})$)	$\dot{H}_{in,p}$	— enthalpy of the permeate inflow (W)
D	— diffusion coefficient for vapor (m^2/s)	$\dot{H}_{out,f}$	— enthalpy of the feed outflow (W)
d	— flow hydraulic diameter (m)	$\dot{H}_{out,p}$	— enthalpy of the permeate outflow (W)
d_p	— membrane pore size (m)	I	— solar irradiation (W/m^2)
ECR	— energy efficiency change rate (s^{-1})	J	— mass flux ($\text{kg}/(\text{m}^2 \text{ s})$)
$EEEC_m$	— specific equivalent electrical energy consumption per unit mass of the product (J/kg)	J_j	— fluxes
$EEEC_V$	— specific equivalent electrical energy consumption per unit volume of the product (J/m^3)	J_v	— volumetric flux (m/s)
\dot{E}	— rate of the exergy transferred (W)	\bar{J}_v	— average volumetric flux (m/s)
\dot{E}^C	— rate of the chemical exergy transferred (W)	k_B	— Boltzman constant (J/K)
\dot{E}_{des}	— exergy destruction rate (W)	k_f	— thermal conductivity of the fluid ($\text{W}/(\text{m K})$)
$\dot{E}_{electrical}$	— rate of the electrical exergy transferred (W)	k_g	— thermal conductivity of the gas present in the pores ($\text{W}/(\text{m K})$)
\dot{E}_{flow}	— rate of the flow exergy transferred (W)	k_m	— effective membrane thermal conductivity ($\text{W}/(\text{m K})$)
$\dot{E}_{in,c}$	— flow exergy of the coolant inflow (W)	Kn	— Knudsen number (dimensionless)
$\dot{E}_{in,f}$	— flow exergy of the feed inflow (W)	k_s	— membrane material thermal conductivity ($\text{W}/(\text{m}^2 \text{ K})$)
$\dot{E}_{in,g}$	— flow exergy of the sweeping gas inflow (W)	k_{so}	— mass transfer coefficient of the solutes (m/s)
$\dot{E}_{in,p}$	— flow exergy of the permeate inflow (W)	L'_{11}	— temperature driven heat flux kinetic coefficient ($\text{W}/(\text{m K})$)
\dot{E}_{input}	— exergy input rate (W)	L'_{12}	— concentration driven heat flux kinetic coefficient ($(\text{W m}^2)/\text{mol}$)
$\dot{E}_{out,c}$	— flow exergy of the coolant outflow (W)	L'_{21}	— temperature driven mass flux kinetic coefficient ($(\text{kg K})/(\text{m s})$)
$\dot{E}_{out,d}$	— flow exergy of the distillate (W)	L'_{22}	— concentration driven mass flux kinetic coefficient ($(\text{kg m}^2)/(\text{mol s})$)
$\dot{E}_{out,f}$	— flow exergy of the feed outflow (W)	L_{11}	— inverse temperature driven heat flux kinetic coefficient ($(\text{K W})/\text{m}$)
$\dot{E}_{out,g}$	— flow exergy of the sweeping gas outflow (W)	L_{12}	— chemical potential driven heat flux kinetic coefficient ($(\text{K kg})/(\text{m s})$)
$\dot{E}_{out,p}$	— flow exergy of the permeate outflow (W)	L_{21}	— inverse temperature driven mass flux kinetic coefficient ($(\text{K kg})/(\text{m s})$)
\dot{E}_{output}	— exergy output rate (W)	L_{22}	— chemical potential driven mass flux kinetic coefficient ($(\text{K kg}^2)/(\text{m s J})$)
\dot{E}^P	— rate of the physical exergy transferred (W)	LEP	— liquid entry pressure (Pa)
\dot{E}_p	— useful exergy output rate (W)	L_{jk}	— kinetic (phenomenological) coefficients
$\dot{E}_{thermal}$	— rate of the thermal exergy transferred (W)	l_p	— average length of the pores (m)
\dot{E}_u	— paid exergy input rate (W)	lr_{sub}	— subprocess relative energy loss to the environment (dimensionless)
e_i	— specific flow exergy of stream i (kJ/kg)	M	— molecular weight of vapor material (kg/mol)
\dot{e}_{sun}	— exergy of the solar irradiation per unit area (W/m^2)	MCR	— mass flux change rate (h^{-1})
$FESR$	— fuel energy saving ratio (dimensionless)		
FR	— foulants rate (s^{-1})		
g	— gravitational acceleration (m/s^2)		
GOR	— gain output ratio (dimensionless)		
h	— convective heat transfer coefficient for fluid flow ($\text{W}/(\text{m}^2 \text{ K})$)		
H	— specific enthalpy (J/kg)		
$H_{d,i}$	— specific enthalpy of the superheated distillate (J/kg)		

m_t	— mass of the solution (kg)	$SEEC_v$	— specific electrical energy consumption per unit volume of the distillate (J/m ³)
m_{sp}	— mass of the species (kg)	SHC_m	— specific heat consumption per unit mass of the distillate (J/kg)
\dot{m}	— mass flow rate (kg/s)	SHC_v	— specific heat consumption per unit volume of the distillate (J/m ³)
$\dot{m}_{in,f}$	— mass inflow rate of the feed solution (kg/s)	SXC_m	— specific exergy consumption per unit mass of the product (J/kg)
$\dot{m}_{in,p}$	— mass inflow rate of the permeate (kg/s)	SXC_{min}	— minimum specific exergy consumption per unit mass of the product (J/kg)
$\dot{m}_{out,f}$	— the mass outflow rate of the feed solution (kg/s)	SXC_v	— specific exergy consumption per unit volume of the product (J/m ³)
$\dot{m}_{out,p}$	— the mass outflow rate of the permeate (kg/s)	T	— temperature (K)
n	— number of the microorganisms per unit area (m ⁻²)	T_{in}	— temperature of the heat input (K)
N	— mole number of the species (mol)	T_v^*	— saturation temperature of the vacuum side's vapor pressure (K)
N_{so}	— mole number of the solutes (mol)	t	— time period (s)
Nu	— Nusselt number (dimensionless)	T_b	— temperature in the bulk of the flow (K)
n_{sol}	— solvent concentration (mol/kg)	TCR	— membrane thickness change rate (s ⁻¹)
P	— pressure (Pa)	T_{inter}	— temperature of the flow at the heat transfer boundary (K)
p	— vapor pressure (Pa)	T_{out}	— temperature of the heat output (K)
p^*	— vapor pressure of pure solvent (Pa)	T_p^*	— saturation temperature of vapor pressure at bulk of the sweeping gas side (K)
p_{air}	— average partial pressure of the non-condensable gas in the membrane (Pa)	$T_{p,m}^*$	— saturation temperature of vapor pressure at the membrane surface of the sweeping gas side (K)
PCR	— product quality change rate (s ⁻¹)	TPC	— temperature polarization coefficient (dimensionless)
PF	— mass transport pre-factor ((m ⁻¹) for $\beta = 0$, (dimensionless) for $\beta = 1$, (m) for $\beta = 2$)	v	— velocity of the fluid flow (m/s)
P_{in}	— flow pressure at the defined flow inlet (Pa)	V	— volume of the solution (m ³)
P_{out}	— flow pressure at the defined flow outlet (Pa)	V_{mem}	— total volume of the membrane (m ³)
PPC	— vapor pressure polarization coefficient (dimensionless)	V_p	— volume of the pores (m ³)
PR	— performance ratio (dimensionless)	\dot{V}	— volumetric flow rate (m ³ /s)
\dot{Q}	— rate of the heat transferred (W)	\dot{W}_e	— rate of the electrical energy transferred (W)
\dot{Q}_e	— heat exchange rate in the condenser (W)	$\dot{W}_{e,b}$	— the electrical energy consumption of the sweeping gas blower (W)
\dot{Q}_{fuel}	— heat input rate by the fuel (W)	$\dot{W}_{e,c}$	— electrical energy consumption of the coolant flow pump (W)
\dot{Q}_{in}	— heat input rate (W)	$\dot{W}_{e,f}$	— electrical energy consumption of the feed flow pump (W)
\dot{Q}_{out}	— heat output rate (W)	$\dot{W}_{e,in}$	— total electrical energy input (W)
\dot{Q}_r	— heat recovery rate (W)	$\dot{W}_{e,p}$	— electrical energy consumption of the permeate flow pump (W)
q''	— heat flux (W/m ²)	$\dot{W}_{e,t}$	— electrical energy output of the vapor power system (W)
q''_c	— heat flux across the membrane by conduction (W/m ²)	$\dot{W}_{e,v}$	— electrical energy consumption of the vacuum pump (W)
q''_t	— total heat flux (W/m ²)	$\dot{W}_{e,w}$	— electrical energy consumption of the water pump (W)
q''_v	— heat flux across the membrane by evaporation (W/m ²)	W_{min}	— minimum work of separation (J/kg)
r	— average pore radius (m)	w	— mass fraction (dimensionless)
R	— rejection factor (dimensionless) or the ideal gas constant (J/(mol K))	x	— mole fraction (dimensionless)
R_c	— heat transfer resistances of the cooling plate ((m ² K)/W)	XDR	— relative exergy destruction ratio (dimensionless)
R_f	— heat transfer resistances of the condensate liquid film ((m ² K)/W)		
R_g	— heat transfer resistances of the air gap ((m ² K)/W)		
R_v	— the gas constant of vapor, defined in Eq. (37) (J/(kg K))		
r_{max}	— largest pore radius (m)		
S	— salinity (%)		
s	— specific entropy of the solution (J/(kg K))		
\dot{s}	— entropy production rate (W/(K m ³))		
$SEEC_m$	— specific electrical energy consumption per unit mass of the distillate (J/kg)		

XCR	— exergy consumption ratio (dimensionless)
X_k	— driving forces
XSR	— exergy saving ratio (dimensionless)
x_{sol}	— molar fraction of solvent (dimensionless)
z	— height of the fluid (m)
	—
<i>Greek</i>	
α	— separation factor (dimensionless)
β	— exponential factor depends on the mass transport mechanism. For the Knudsen diffusion mechanism, $\beta = 1$; for the viscous flow mechanism, $\beta = 2$; for the ordinary molecular diffusion mechanism, $\beta = 0$
γ	— activity coefficient (dimensionless)
γ_L	— liquid surface tension (N/m)
δ	— membrane thickness (m)
ΔH_{fg}	— specific enthalpy of vaporization (J/kg)
ΔP	— flow pressure drop (Pa)
ΔP_{inter}	— pressure difference at liquid/gas interface (Pa)
ε	— membrane porosity (dimensionless)
η	— membrane thermal efficiency (dimensionless)
$\eta_{e,dual}$	— the heat to electrical energy conversion factor for the dual-purpose desalination plant (dimensionless)
$\eta_{e,ref}$	— heat to electrical energy conversion factor for the reference power plant (dimensionless)
η_{sc}	— energy efficiency of the solar collector (dimensionless)
$\eta_{w,ref}$	— heat to water conversion factor for the reference desalination plant (kg/J)
θ	— membrane/liquid contact angle ($^\circ$ or rad)
λ	— mean free path of vapor (m)
μ	— viscosity of vapor (Pa s) or chemical potential (J/kg)
$\xi_{e,ref}$	— exergy to electrical energy conversion factor for the reference power plant (dimensionless)
$\xi_{w,ref}$	— exergy to water conversion factor for the reference desalination plant (kg/J)
ρ	— density (kg/m ³)
ρ_f	— density of the fluid (kg/m ³)
ρ_{mat}	— density of the membrane solid matrix material (kg/m ³)
σ	— collision diameter of the molecule (m)
τ	— membrane tortuosity (dimensionless)
ψ_t	— overall exergy efficiency (dimensionless)
ψ_u	— utilitarian exergy efficiency (dimensionless)

Superscripts

flu	— solar irradiation exergy and related value based on the temperature of the fluid, referred Eq. (135)
h	— heat exchanger
m	— membrane module
sun	— solar irradiation exergy and related value based on the temperature of the sun, referred Eq. (134)

Subscripts

0	— dead state
$coup$	— distillate
d	— distillate
$dual$	— dual-purpose desalination plant
f,m	— membrane feed side-surface
f	— feed stream bulk
f	— feed solution
$final$	— final value
i	— species i or stream i
$intial$	— initial value
j	— subsystem or subprocess j
MD	— reference MD system
me	— mean value
mem	— membrane
oth	— reference system conducts only the ‘other process’ coupled with MD
pow	— reference power-only system
pro	— product
p,m	— membrane permeate-side surface
p	— permeate stream bulk
PV	— PV module
s	— steam
sc	— solar collector
sun	— sun
sub	— subsystem
wat	— reference water-only system

References

- [1] A.M. Alklaibi, N. Lior, Membrane-distillation desalination: Status and potential, *Desalination* 171 (2005) 111–131.
- [2] A. Alkhdhiri, N. Darwish, N. Hilal, Membrane distillation: A comprehensive review, *Desalination* 287 (2012) 2–18.
- [3] P. Wang, T. Chung, Recent advances in membrane distillation processes: Membrane development, configuration design and application exploring, *J. Membr. Sci.* 474 (2015) 39–56.
- [4] M.S. El-Bourawi, Z. Ding, R. Ma, M. Khayet, A framework for better understanding membrane distillation separation process, *J. Membr. Sci.* 285 (2006) 4–29.
- [5] K.W. Lawson, D.R. Lloyd, Membrane distillation, *J. Membr. Sci.* 124 (1997) 1–25.
- [6] M.M.A. Shirazi, A. Kargari, A review on application of membrane distillation (MD) process for wastewater treatment, *J. Memb. Sci. Res.* 1 (2015) 101–112.
- [7] L.M. Camacho, L. Dumée, J. Zhang, J. Li, M. Duke, J. Gomez, S. Gray, Advances in membrane distillation for water desalination and purification applications, *Water (Switzerland)* 5 (2013) 94–196.
- [8] E. Drioli, A. Ali, F. Macedonio, Membrane distillation: Recent developments and perspectives, *Desalination* 356 (2015) 56–84.
- [9] M. Khayet, Membrane distillation, *Adv. Membr. Technol. Appl.* (2008) 297–369.

- [10] E. Curcio, E. Drioli, Membrane distillation and related operations—A review, *Sep. Purif. Rev.* 34 (2005) 35–86.
- [11] M. Khayet, Membranes and theoretical modeling of membrane distillation: A review, *Adv. Colloid Interface Sci.* 164 (2011) 56–88.
- [12] W.M. Haynes, *CRC Handbook of Chemistry and Physics*, CRC Press, Boca Raton, FL, 2014.
- [13] S.L. Clegg, K.S. Pitzer, Thermodynamics of multicomponent, miscible, ionic solutions: Generalized equations for symmetrical electrolytes, *J. Phys. Chem.* 96 (1992) 3513–3520.
- [14] S.L. Clegg, K.S. Pitzer, P. Brimblecombe, Thermodynamics of multicomponent, miscible, ionic solutions. Mixtures including unsymmetrical electrolytes, *J. Phys. Chem.* 96 (1992) 9470–9479.
- [15] L. Fitzsimons, B. Corcoran, P. Young, G. Foley, Exergy analysis of water purification and desalination: A study of exergy model approaches, *Desalination* 359 (2015) 212–224.
- [16] K.H. Mistry, J.H.V. Lienhard, Effect of nonideal solution behavior on desalination of a sodium chloride solution and comparison to seawater, *J. Energy Resour. Technol. Trans. ASME* 135 (2013) 4.
- [17] K.H. Mistry, H.A. Hunter, Effect of composition and nonideal solution behavior on desalination calculations for mixed electrolyte solutions with comparison to seawater, *Desalination* 318 (2013) 34–47.
- [18] S. Hwang, Nonequilibrium thermodynamics of membrane transport, *Desalination* 50 (2004) 862–870.
- [19] F.A. Banat, J. Simandl, Theoretical and experimental study in membrane distillation, *Desalination* 95 (1994) 39–52.
- [20] L. Wang, J. Min, Modeling and analyses of membrane osmotic distillation using non-equilibrium thermodynamics, *J. Membr. Sci.* 378 (2011) 462–470.
- [21] K.H. Mistry, R.K. McGovern, G.P. Thiel, E.K. Summers, S.M. Zubair, J.H. Lienhard, Entropy generation analysis of desalination technologies, *Entropy* 13 (2011) 1829–1864.
- [22] Y. Wang, N. Lior, Fuel allocation in a combined steam-injected gas turbine and thermal seawater desalination system, *Desalination* 214 (2007) 306–326.
- [23] A.M. El-Nashar, Cogeneration for power and desalination—State of the art review, *Desalination* 134 (2001) 7–28.
- [24] G.P. Maheshwari, M. Al-Ramadhan, M. Al-Abdulhadi, Energy requirement of water production in dual-purpose plants, *Desalination* 101 (1995) 133–140.
- [25] L. Yang, S. Shen, Assessment of energy requirement for water production at dual-purpose plants in China, *Desalination* 205 (2007) 214–223.
- [26] I. Kamal, Integration of seawater desalination with power generation, *Desalination* 180 (2005) 217–229.
- [27] W.R. Dunbar, N. Lior, R.A. Gaggioli, Component equations of energy and exergy, *J. Energy. Resour. Technol., Trans. ASME* 114 (1992) 75–83.
- [28] K. Smolders, A.C.M. Franken, Terminology for membrane distillation, *Desalination* 72 (1989) 249–262.
- [29] M. Khayet, A. Velázquez, J.I. Mengual, Modelling mass transport through a porous partition: Effect of pore size distribution, *J. Non Equilib. Thermodyn.* 29 (2004) 279–299.
- [30] L. Martínez, F.J. Florido-Díaz, A. Hernandez, P. Pradanos, Estimation of vapor transfer coefficient of hydrophobic porous membranes for applications in membrane distillation, *Sep. Purif. Technol.* 33 (2003) 45–55.
- [31] N. Lior, *Measurements and Control in Water Desalination*, Elsevier, Amsterdam, 1986.
- [32] ASTM D4419-90(2015), Standard Test Method for Measurement of Transition Temperatures of Petroleum Waxes by Differential Scanning Calorimetry (DSC), ASTM International, West Conshohocken, PA, 2015. Available from: <www.astm.org>.
- [33] ASTM E2105-00(2010), Standard Practice for General Techniques of Thermogravimetric Analysis (TGA) Coupled With Infrared Analysis (TGA/IR), ASTM International, West Conshohocken, PA, 2010. Available from: <www.astm.org>.
- [34] M.H. Sharqawy, J.H. Lienhard, S.M. Zubair, Thermophysical properties of seawater: A review of existing correlations and data, *Desal. Wat. Treat.* 16 (2010) 354–380.
- [35] R.W. Schofield, A.G. Fane, C.J.D. Fell, R. Macoun, Factors affecting flux in membrane distillation, *Desalination* 77 (1990) 279–294.
- [36] R.W. Schofield, A.G. Fane, C.J.D. Fell, Gas and vapour transport through microporous membranes. II. Membrane distillation, *J. Membr. Sci.* 53 (1990) 173–185.
- [37] L.F. Dumée, S. Gray, M. Duke, K. Sears, J. Schütz, N. Finn, The role of membrane surface energy on direct contact membrane distillation performance, *Desalination* 323 (2013) 22–30.
- [38] G.C. Sarti, C. Gostoli, S. Bandini, Extraction of organic components from aqueous streams by vacuum membrane distillation, *J. Membr. Sci.* 80 (1993) 21–33.
- [39] Y. Fujii, S. Kigoshi, H. Iwatani, M. Aoyama, Selectivity and characteristics of direct contact membrane distillation type experiment. I. Permeability and selectivity through dried hydrophobic fine porous membranes, *J. Membr. Sci.* 72 (1992) 53–72.
- [40] Y. Fujii, S. Kigoshi, H. Iwatani, M. Aoyama, Y. Fusaoka, Selectivity and characteristics of direct contact membrane distillation type experiment. II. Membrane treatment and selectivity increase, *J. Membr. Sci.* 72 (1992) 73–89.
- [41] M.A. Izquierdo-Gil, G. Jonsson, Factors affecting flux and ethanol separation performance in vacuum membrane distillation (VMD), *J. Membr. Sci.* 214 (2003) 113–130.
- [42] F.A. Banat, J. Simandl, Membrane distillation for dilute ethanol: Separation from aqueous streams, *J. Membr. Sci.* 163 (1999) 333–348.
- [43] M.J. Moran, H.N. Shapiro, D.D. Boettner, M.B. Bailey, *Fundamentals of Engineering thermodynamics*, John Wiley & Sons, Hoboken, NJ, 2014.
- [44] J. Szargut, *Exergy Method: Technical and Ecological Applications*, WIT Press, Southampton, 2005.
- [45] N. Lior, N. Zhang, Energy, exergy, and Second Law performance criteria, *Energy* 32 (2007) 281–296.
- [46] S. Al-Obaidani, E. Curcio, F. Macedonio, G. Di Profio, H. Al-Hinai, E. Drioli, Potential of membrane distillation in seawater desalination: Thermal efficiency, sensitivity study and cost estimation, *J. Membr. Sci.* 323 (2008) 85–98.
- [47] F. Macedonio, E. Curcio, E. Drioli, Integrated membrane systems for seawater desalination: Energetic and exergetic analysis, economic evaluation, experimental study, *Desalination* 203 (2007) 260–276.

- [48] F. Banat, N. Jwaied, Exergy analysis of desalination by solar-powered membrane distillation units, *Desalination* 230 (2008) 27–40.
- [49] M.H. Sharqawy, J.H. Lienhard V, S.M. Zubair, On exergy calculations of seawater with applications in desalination systems, *Int. J. Therm. Sci.* 50 (2011) 187–196.
- [50] H. Hong, H. Jin, J. Ji, Z. Wang, R. Cai, Solar thermal power cycle with integration of methanol decomposition and middle-temperature solar thermal energy, *Solar Energy* 78 (2005) 49–58.
- [51] J. Phattaranawik, R. Jiraratananon, A.G. Fane, Heat transport and membrane distillation coefficients in direct contact membrane distillation, *J. Membr. Sci.* 212 (2003) 177–193.
- [52] M. Qtaishat, T. Matsuura, B. Kruczek, M. Khayet, Heat and mass transfer analysis in direct contact membrane distillation, *Desalination* 219 (2008) 272–292.
- [53] A.S. Alsaadi, L. Francis, G.L. Amy, N. Ghaffour, Experimental and theoretical analyses of temperature polarization effect in vacuum membrane distillation, *J. Membr. Sci.* 471 (2014) 138–148.
- [54] D.M. Warsinger, J. Swaminathan, E. Guillen-Burrieza, H.A. Arafat, J.H. Lienhard V, Scaling and fouling in membrane distillation for desalination applications: A review, *Desalination* 356 (2015) 294–313.
- [55] J. Schwinge, P.R. Neal, D.E. Wiley, D.F. Fletcher, A.G. Fane, Spiral wound modules and spacers: Review and analysis, *J. Membr. Sci.* 242 (2004) 129–153.
- [56] L. Martínez-Díez, M.I. Vázquez-González, Temperature and concentration polarization in membrane distillation of aqueous salt solutions, *J. Membr. Sci.* 156 (1999) 265–273.
- [57] R.G. Raluy, R. Schwantes, V.J. Subiela, B. Peñate, G. Melián, J.R. Betancort, Operational experience of a solar membrane distillation demonstration plant in Pozo Izquierdo-Gran Canaria Island (Spain), *Desalination* 290 (2012) 1–13.
- [58] B. Li, K.K. Sirkar, Novel membrane and device for direct contact membrane distillation-based desalination process, *Ind. Eng. Chem. Res.* 43 (2004) 5300–5309.
- [59] F. Banat, N. Jwaied, M. Rommel, J. Koschikowski, M. Wieghaus, Desalination by a “compact SMADES” autonomous solarpowered membrane distillation unit, *Desalination* 217 (2007) 29–37.
- [60] K. He, H.J. Hwang, M.W. Woo, I.S. Moon, Production of drinking water from saline water by direct contact membrane distillation (DCMD), *J. Ind. Eng. Chem.* 17 (2011) 41–48.
- [61] X. Wang, L. Zhang, H. Yang, H. Chen, Feasibility research of potable water production via solar-heated hollow fiber membrane distillation system, *Desalination* 247 (2009) 403–411.
- [62] M. Gryta, Desalination of thermally softened water by membrane distillation process, *Desalination* 257 (2010) 30–35.
- [63] M. Gryta, Alkaline scaling in the membrane distillation process, *Desalination* 228 (2008) 128–134.
- [64] M. Gryta, M. Tomaszewska, K. Karakulski, Wastewater treatment by membrane distillation, *Desalination* 198 (2006) 67–73.
- [65] S.T. Hsu, K.T. Cheng, J.S. Chiou, Seawater desalination by direct contact membrane distillation, *Desalination* 143 (2002) 279–287.
- [66] E. Guillen-Burrieza, R. Thomas, B. Mansoor, D. Johnson, N. Hilal, H. Arafat, Effect of dry-out on the fouling of PVDF and PTFE membranes under conditions simulating intermittent seawater membrane distillation (SWMD), *J. Membr. Sci.* 438 (2013) 126–139.
- [67] L.D. Tijing, Y.C. Woo, J. Choi, S. Lee, S. Kim, H.K. Shon, Fouling and its control in membrane distillation—A review, *J. Membr. Sci.* 475 (2015) 215–244.
- [68] H. Shon, S. Phuntsho, S. Vigneswaran, J. Kandasamy, R. Aryal, V. Jegatheesan, Physical, chemical, and biological characterization of membrane fouling, *Membr. Technol. Environ. Appl.* (2012) 457–503.
- [69] S. Phuntsho, A. Listowski, H.K. Shon, P. Le-Clech, S. Vigneswaran, Membrane autopsy of a 10 year old hollow fibre membrane from Sydney Olympic Park water reclamation plant, *Desalination* 271 (2011) 241–247.